

22009

National Library
of CanadaBibliothèque nationale
du CanadaCANADIAN THESES
ON MICROFICHETHÈSES CANADIENNES
SUR MICROFICHE

NAME OF AUTHOR/NOM DE L'AUTEUR

Richard William Wilton

TITLE OF THESIS/TITRE DE LA THÈSE

Some Infrared and X-ray Properties
of the High Pressure Polymorph
of Solid Acetic Acid

UNIVERSITY/UNIVERSITÉ

U. of A.

DEGREE FOR WHICH THESIS WAS PRESENTED/

GRADE POUR LEQUEL CETTE THÈSE FUT PRÉSENTÉE

M. Sc.

YEAR THIS DEGREE CONFERRED/ANNÉE D'OBTENTION DE CE DEGRÉ

1974

NAME OF SUPERVISOR/NOM DU DIRECTEUR DE THÈSE

Dr. J.E. Bertie

Permission is hereby granted to the NATIONAL LIBRARY OF
CANADA to microfilm this thesis and to lend or sell copies
of the film.

The author reserves other publication rights, and neither the
thesis nor extensive extracts from it may be printed or other-
wise reproduced without the author's written permission.

L'autorisation est, par la présente, accordée à la BIBLIOTHÈ-
QUE NATIONALE DU CANADA de microfilmer cette thèse et
de prêter ou de vendre des exemplaires du film.

L'auteur se réserve les autres droits de publication; ni la
thèse ni de longs extraits de celle-ci ne doivent être imprimés
ou autrement reproduits sans l'autorisation écrite de l'auteur.

DATED/DATÉ

Sept 27/74

SIGNED/SIGNÉ

R. Wilton

PERMANENT ADDRESS/RÉSIDENCE FIXE

Box 125 Stn. F

Winnipeg, Man.

R2L 2A50

THE UNIVERSITY OF ALBERTA

SOME INFRARED AND X-RAY PROPERTIES OF THE
HIGH PRESSURE POLYMORPH OF SOLID ACETIC ACID

by



RICHARD W. WILTON

A THESIS

SUBMITTED TO THE FACULTY OF GRADUATE STUDIES AND RESEARCH
IN PARTIAL FULFILMENT OF THE REQUIREMENTS FOR THE DEGREE

OF

MASTER OF SCIENCE

DEPARTMENT OF CHEMISTRY

EDMONTON, ALBERTA

FALL, 1974

THE UNIVERSITY OF ALBERTA
FACULTY OF GRADUATE STUDIES AND RESEARCH

The undersigned certify that they have read,
and recommend to the Faculty of Graduate Studies and
Research, for acceptance, a thesis entitled
Infrared and X-ray Properties of the High Pressure
Polymorph of Solid Acetic Acid
submitted by Richard W. Wilton
in partial fulfilment of the requirements for the degree
of Master of Science

..... John E. Bert
Supervisor
Frank R. Werh
.....
.....

Date September 26, 1974

To my Father

Abstract

The low temperature, high pressure phase of solid acetic acid has been studied using X-ray and infrared techniques. The pressure-temperature phase diagram of acetic acid has been measured between 0 and -40°C to 3 Kbar using volume discontinuity as the indicator of the pressure at which the phase transition occurred at a certain temperature. The equilibrium transition pressure is given as the average of the pressures required for the acetic acid I \rightarrow II and acetic acid II \rightarrow I transitions. It was found that acetic acid II cannot be formed from acetic acid I below about 800 bar, even though it appears to be the stable phase at one atmosphere below about -60°C . However, once it is formed, acetic acid II is metastable at one atmosphere below about -35°C . The acetic acid I \rightarrow II transition is accompanied by a $0.014\text{ cm}^3/\text{g}$ decrease in volume.

The X-ray diffraction pattern of powdered acetic acid II has been obtained and indexed on a monoclinic cell with the dimensions: $a = 13.30 \pm 0.02\text{ \AA}$, $b = 10.39 \pm 0.01\text{ \AA}$, $c = 8.59 \pm 0.01\text{ \AA}$ and $\beta = 86.1 \pm 0.3^{\circ}$ at 100°K and atmospheric pressure. If the unit cell contains 16 molecules, the molar volume is $44.6\text{ cm}^3/\text{mole}$, 1.5% smaller than that of acetic acid I, in agreement with the results from the phase diagram work.

The far infrared spectrum of acetic acid II has been obtained and compared to those of acetic acid I and propionic acid. It has been argued that acetic acid II probably consists of hydrogen-bonded chains of monomers which are packed in a more efficient way than in acetic acid I.

Acknowledgements

I have a deep and sincere appreciation for Dr. J.E. Bertie. It was a privilege to work under his direction, and his guidance, encouragement and understanding were invaluable during the course of this work.

I also wish to express my appreciation to the other members of this department, especially those in Dr. Bertie's research group, for their interest, co-operation and helpful discussions. Particular thanks must go to the members of the machine shop and electronics shop for their prompt and competent workmanship in building and maintaining equipment used in this work.

Many friends outside the chemistry department have also been very helpful by expressing interest and encouragement during this work. Among these I would especially like to thank my family, Larry Whitehouse and Mac Jardine.

Financial support of this work by the University of Alberta is gratefully acknowledged.

Table of Contents

Chapter	Page
1. Introduction.....	1
1A. General Introduction	1
1B. Previous Reports of Polymorphism in Solid Acetic Acid	2
1C. A Review of the Physical Properties of Acetic Acid at Atmospheric Pressure	8
1D. A Review of the Low Frequency Vibrational Spectra of Acetic Acid and Related Compounds	14
1E. Objectives of this work	36
2. Experimental	38
2A. Purification of Chemicals	38
2B. Apparatus and Sample Handling Methods for the Phase Diagram Measurements	41
2C. Preparation of Acetic Acid II and Ground Samples	47
2D. X-ray Experimental and Method	50
2E. Spectroscopic Methods	53

Chapter	Page
3. The Phase Diagram of Acetic Acid Below 0°C	62
3A. Methods	62
3B. Results and Discussion of the Phase Diagram Work	68
4. A Discussion of the X-ray Measurements on Acetic Acid Powdered Solids	76
5. The Far Infrared Spectra of Acetic Acid I, Acetic Acid II and Propionic Acid	88
5A. Analysis of the Inter-monomer Vibrations of Acetic Acid I	88
5B. Far Infrared Spectra Obtained	97
5C. Discussion of the Spectra	105
5D. Summary and Conclusions	109
References	111

List of Tables

Table	Description	Page
1.	Melting points of acetic acid	4
2.	Corrected melting points of acetic acid.....	4
3.	Refractive index of acetic acid for seven different light sources.....	12
4.	Low frequency vibrations observed and calculated for acetic acid dimer and its deuterated analogs	19
5.	Lattice vibrations of propionic acid	33
6.	Observed frequencies and assignments for $\text{CH}_3\text{CH}_2\text{COOH}$ and $\text{CD}_3\text{CD}_2\text{COOD}$ solids in the low-frequency region.....	35
7.	Phase diagram of solid acetic acid	69
8.	Thermodynamic parameters for the solid acetic acid phase transition	75
9.	X-ray powder diffraction data for acetic acid I at 100°K and atmospheric pressure....	78
10.	X-ray powder diffraction data for acetic acid II at 100°K and atmospheric pressure..	80
11.	Powder diffraction patterns of acetic acid I at 278 and 83°K , calculated from the cell parameters and structure factors reported by Nahrinbauer (18)	85
12.	Symmetry coordinates of acetic acid I	95
13.	Observed vibrational frequencies of acetic acid I, acetic acid II and propionic acid	101

List of Figures

Figure	Page
1. Symmetry coordinates and vibrations of carboxylic acid dimers.....	17
2. The high pressure cell used for the phase diagram studies.....	42
3. High pressure cell used to prepare and recover acetic acid II.....	48
4. The cell used for low temperature infrared spectra.....	54
5. Graph of volume change <u>vs.</u> pressure for the phase transition occurring at 0°C.....	65
6. Graph of volume change <u>vs.</u> pressure for the phase transition occurring at 0°C.....	66
7. Graph of volume change <u>vs.</u> pressure for the phase transition occurring at 0°C.....	67
8. The pressure-temperature phase diagram of solid acetic acid.....	71
9. Symmetry coordinates for a single chain of acetic acid I.....	91
10. The far infrared spectrum of polycrystalline acetic acid I at approximately -180°C.....	98
11. The far infrared spectrum of polycrystalline acetic acid II at approximately -180°C.....	99
12. The far infrared spectrum of polycrystalline propionic acid at approximately -180°C.....	100

Chapter I. Introduction

1A. General Introduction

Although acetic acid is a very commonplace, widely used chemical, data concerning the physical properties of its second polymorphic solid phase are almost nonexistent. Even the fact that acetic acid is capable of existing in two solid phases is almost unknown. For example, a recent paper on the infrared spectrum of acetic acid under pressure (1) reported that at least two polymorphic forms had been detected, with no reference to the fact that the existence of two polymorphic forms has been known for 70 years. Following Tammann (2) and Bridgman (3), the solid polymorph which is well known at atmospheric pressure is called acetic acid I, while the phase which forms at about 1 Kbar pressure at 0°C is called acetic acid II.

This thesis presents a study of the phase diagram of acetic acid below 0°C to 3 Kbar, the X-ray powder pattern of acetic acid II at atmospheric pressure and about 100°K, and the far infrared spectrum of acetic acid II at atmospheric pressure and 100°K. These results are presented and discussed in Chapters 3, 4 and 5 and the experimental methods are described in Chapter 2. The literature on polymorphism in solid acetic acid is reviewed in Section 1B, while the more general physical properties of acetic acid are discussed in Section 1C. Previous

studies of the far infrared spectra of acetic acid and other relevant carboxylic acids are discussed in Section 1D and the objectives of the present work are stated in Section 1E.

In Chapter 1 many different pressure units are used, following the usage of the authors cited. The relation between these various units is given below:

$$1 \text{ bar} = 0.001 \text{ Kbar} = 1.0197 \text{ Kg cm}^{-2} = 0.9862 \text{ atmosphere} \\ = 749.5 \text{ torr}$$

1B. Previous Reports of Polymorphism in Solid Acetic Acid

The first report of acetic acid II was made by G. Tammann (2) in 1903. Tammann recorded the pressure-temperature phase diagram of acetic acid to a pressure of 3000 Kg cm^{-2} over the temperature range -20.7 to $+65^\circ\text{C}$, and found three transition lines, liquid-solid I, liquid-solid II and solid I - solid II. He reported the triple point for the equilibrium between these three phases as 57.5°C and 2330 Kg cm^{-2} and that at the lowest temperature on his phase diagram, -20.7°C , acetic acid II formed from acetic acid I at 765 Kg cm^{-2} . Tammann reported that the solid-solid phase transition occurred at -71°C at atmospheric pressure but he did not give any experimental details, and it is assumed that he formed

acetic acid II at high pressure, cooled it before lowering the pressure and then observed the phase transition as it warmed up at atmospheric pressure.

P. W. Bridgman (3) in 1916 reported the phase diagram for acetic acid up to $12,000 \text{ Kg cm}^{-2}$ from 0°C to 165°C . At higher temperatures and pressures the chemical reaction between the acetic acid and the steel pressure vessel was so fast that the sample became too impure for the results to be useful. Bridgman used three samples of acetic acid and found the phase transition lines to be somewhat shifted from the temperatures and pressures reported by Tammann (2); however he explained the difference by claiming that his samples were of higher purity than Tammann's. Bridgman tabulated his data and thermodynamic parameters for the liquid-acetic acid I-acetic acid II phase transitions, with the liquid-solid I - solid II triple point at 55.7°C and $2100^\circ \text{Kg cm}^{-2}$ and phase II forming from phase I at 1074 Kg cm^{-2} at 0° .

In 1935 Louis Deffet (4) measured the melting curve for acetic acid up to 1000 Kg cm^{-2} . Deffet's results agreed better with those of Tammann (2) than with Bridgman's (3). Table 1 presents the melting points observed by these workers over the pressure range $1 - 1000 \text{ Kg/cm}^2$, and includes the accepted value of the melting point at atmospheric pressure (5). When the melting points at 1 Kg/cm^2 are corrected to 16.604°C and

Table 1. Melting Points of Acetic Acid

	<u>1 Kg/cm²</u>	<u>500 Kg/cm²</u>	<u>1000 Kg/cm²</u>
Tammann (2)	16.65°C	27.1°C	37.05°C
Bridgman (3)	16.68°C	27.8°C	37.7°C
Deffet (4)	16.55°C	26.7°C	36.9°C
Beilstein (5)	16.604°C		

Table 2. Corrected Melting Points of Acetic Acid

	<u>1 Kg/cm² correction</u>	<u>500 Kg/cm²</u>	<u>1000 Kg/cm²</u>
Tammann (2)	-0.046°C	27.06°C	37.00°C
Bridgman (3)	-0.076°C	27.72°C	37.62°C
Deffet (4)	+0.054°C	26.75°C	36.95°C
Beilstein (5)	0.000°C		

equal corrections are made for the melting points at higher pressure, as shown in Table 2, the values of Tammann and Deffet are in even better agreement but those of Bridgman are significantly higher.

Willy Tan et. al. (6), in 1952, measured the freezing point curve for the acetic acid-benzene system. A definite 'nick' occurred in the curve at 7.28°C and 78.4% acetic acid by weight. The explanation of this irregularity in the curve may be based either on the formation of a compound or on the presence of polymorphism in solid acetic acid. X-ray studies were carried out on the solid obtained at temperatures above and below the temperature of the 'nick', with the conclusion that the 'nick' was due to polymorphism in solid acetic acid. This conclusion was based on the fact that two lines in the powder pattern of the solid obtained at $1-2^{\circ}\text{C}$ were absent in that of the solid obtained at $8-9^{\circ}\text{C}$. However it is interesting to note that these lines were also found in the powder pattern of pure benzene. Further, other lines which coincided with the lines in the benzene pattern were of medium or strong intensity in the powder pattern of the solid obtained at $1-2^{\circ}\text{C}$ and were weak or very weak in that of the solid obtained at $8-9^{\circ}\text{C}$. Thus, although these authors interpreted their results as indicating polymorphism in acetic acid, it is possible that the presence of solid benzene in the solid obtained

at 1-2°C was not realized by them. However, even if their interpretation is correct, it seems unlikely that acetic acid II was the second polymorph involved.

In 1955 Philippe and Piette (7) published measurements of the dielectric constant of acetic acid in the temperature range +20 to -79°C. They were studying the effect of polymorphism on the dielectric constant and reported a solid-solid phase transition in acetic acid at -35°C. Their sample of acetic acid was supplied by the Bureau des Etalons Physico-chimiques but by comparison with similar work done by Raczky et. al. (8), impurity in the sample is suspected to be the cause of the observed phase transition.

Timmermans and Kasanin (9), in 1959, studied the effects of pressure on the melting points of binary systems in which the individual components exhibit polymorphism. The acetic acid-water system and the acetic acid-acetone system were among these studied. The phase diagrams reported by Bridgman were accepted as being correct and their experiments (9) confirmed the existence of polymorphism in solid acetic acid below 3 Kbar.

Raczky, Constant and Gabillard (8) in 1961 measured the dielectric properties at 100 KHz of acetic acid between +20 and -35°C at atmospheric pressure. They also measured the dielectric properties at 1 and 100 KHz of acetic acid contaminated with small amounts of water.

The dielectric constant and loss, ϵ' and ϵ'' , changed markedly at the melting point, as expected, but another marked change was observed at -30°C , which implies that a phase transition occurred at this temperature.

Raczy et. al. made no attempt to interpret these results, since experiments were in progress to measure the complex permittivity as a function of frequency, in the hope that the new data would allow them to state more precisely the nature of the phenomenon observed. Unfortunately the results from those additional experiments have not been published. However, the change observed at -30°C was very small for pure acetic acid, and increased greatly as the water content was raised to 2%, which clearly suggests that it is related to the impurity, and is not an intrinsic property of acetic acid.

The most recent work relating to polymorphism in acetic acid was done in 1967 when Jakobsen, Mikawa and Brasch (1) reported having obtained mid-infrared spectra of at least two polymorphic solid phases in a diamond-windowed high-pressure cell. They did not, however, report the mid-infrared spectra so obtained, but merely reported the far infrared spectrum of the crystal at -150°C and presumably, but not clearly stated atmospheric pressure. The spectrum reported was, therefore, probably of acetic acid I. The mid-infrared spectra which they obtained were later presented at the Symposium on Spectroscopy of

Materials Under High Pressure in 1971 and were published in 1972 (10) with very little explanation.

These are the only published references to polymorphism in acetic acid. It is clear that very little is known about the high pressure phase, acetic acid II.

1C. A Review of the Physical Properties of Acetic Acid at Atmospheric Pressure.

The physical properties of acetic acid have been surveyed by Beilstein (11) and by Timmermans (12). The values given in the 1970 edition of the 'Handbook of Chemistry and Physics' (5) follow Beilstein. In this section some of these physical properties will be discussed with a view to establishing the reliability of its accepted value.

The values reported for the boiling point and the melting point of acetic acid at atmospheric pressure vary considerably, and one problem inherent in the evaluation of these values is that very few workers report how their thermometers were standardized. Bousfield and Lowry (13) reported a melting point of $16.600 \pm 0.005^\circ\text{C}$ using a thermometer calibrated at the National Physical Laboratory in England. Eichelberger and La Mer (14) reported a melting point of $16.60 \pm 0.01^\circ\text{C}$ using a thermometer which had been calibrated against a

Copper-constantan thermocouple, which, in turn was standardized against the fixed points of 0°C and 32.384°C (melting point of $\text{Na}_2\text{SO}_4 \cdot 10\text{H}_2\text{O}$) and against a platinum resistance thermometer certified by the National Bureau of Standards. Both of these melting points are in agreement with the one reported by Schall and Thieme-Wiedtmarckter (15), 16.604°C , which now appears in the 'Handbook of Chemistry and Physics' (5) without a specified accuracy. The boiling temperature is more uncertain than the melting temperature but in the reviews (11, 12) most workers indicate that the boiling point at 760 torr is in the range $117.9 \pm 0.1^{\circ}\text{C}$. The critical point for acetic acid was measured by Young (16) to be at 321.6°C and 43,400 torr.

The density of liquid acetic acid has been measured many times and is $1.0492 \pm 0.0001 \text{ g cm}^{-3}$ at 20°C . The values reported by different workers are usually within 0.01% of this value (11, 12). Young (16) in 1910 and Costello and Bowden (17) in 1958 reported the density of the liquid and vapor from 20°C to temperatures well above the normal boiling point and their values are in very good mutual agreement. Recently the density of acetic acid I was determined from X-ray data to be $1.270 \pm 0.002 \text{ g cm}^{-3}$ (18, 19) at 5°C and $1.334 \pm 0.002 \text{ g cm}^{-3}$ (18) at -190°C .

Eichelberger and La Mer (14) reported a specific conductance of $1.4 \times 10^{-8} \text{ mho cm}^{-1}$ at 25°C . The frequency of the electric field was not given but this value was also reported by MacInnes and Shedlovsky (20), who

found that the specific conductance remained constant over the frequency range 0-3000 Hz. Higher values of specific conductance have been reported by other workers (21, 22), but the value of 1.4×10^{-8} mho cm^{-1} at 25°C is probably the most reliable since impurities tend to increase the conductance.

✓ The dielectric constant is of interest, especially since the results of Raczy et. al. (8) and Philippe and Piette (7) seem to indicate that a solid-solid phase transition occurs between -30 and -35°C. The dielectric constant of Raczy's pure acetic acid measured at 100 KHz was 6.1 to 6.2 in the liquid phase below +20°C and dropped to about 3.6 as the acetic acid solidified. The dielectric constant continued to drop to 3.4 as the temperature was lowered to -30°C and then dropped abruptly to about 3.0 which was the value reported at their lowest temperature, -31°C (8). Philippe and Piette (7) measured the dielectric constant between +20 and -79°C but did not report the frequency at which their measurements were made. However they reported a value of 6.203 at 20°C, decreasing to 6.165 at the melting point where it dropped to about 3.1 during solidification. At -31.5°C they reported a dielectric constant of 2.610 and below the transition at -35.5°C they reported 2.535 with an abrupt change of about 0.1 at approximately -35°C. Since these two reports are so different, not only

in observed dielectric constant but also in the temperature of the transition, nothing can be concluded concerning their reliability.

The dielectric constant of liquid acetic acid was measured by Le Fevre (23) at 2 KHz between 20°C and 80°C. He found the dielectric constant to be 6.170 at 20°C whereas Philippe and Piette (7) reported 6.203. This discrepancy at 20°C suggests that Philippe and Piette may have had some water impurity in their sample. Constant and Lebrun (24) have measured the dielectric constant and loss of liquid acetic acid at 25°C between 0.1 and 100 GHz, and have observed the absorption due to molecular reorientation to be centered at about 2 GHz.

The refractive index of liquid acetic acid for the sodium D line (5893 Å) has been measured by Puschin and Matavulj (25) at 10°C, 25°C, 40°C and 65°C. The values they obtained are: $n_D^{10} = 1.3758$, $n_D^{25} = 1.3698$, $n_D^{40} = 1.3638$ and $n_D^{65} = 1.3537$; $\partial n_D / \partial T$ is, therefore, $-40.0 \times 10^{-5} (\text{°C})^{-1}$ between 10 and 40°C. Dreisbach and Martin (26) report the sodium D line refractive index at 20 and 25°C to be $n_D^{20} = 1.37160$ and $n_D^{25} = 1.36995$, from which $\partial n_D / \partial T$ equals $-33 \times 10^{-5} (\text{°C})^{-1}$ between 20 and 25°C. Another investigation of the refractive index of liquid acetic acid was made using seven different light sources (12) from which the values of n_{15} and $\partial n / \partial T$ were reported as in Table 3.

Table 3. Refractive Index of Acetic Acid For Seven Different Light Sources

Light source ° wave length (Å)	<u>He r</u>	<u>Hα</u>	<u>He y</u>	<u>He g</u>	<u>Hβ</u>	<u>He v</u>	<u>Hγ</u>
	6678.1	6562.8	5875.6	5015.7	4861.3	4471.5	4340.5
n_{15}	1.37131	1.37165	1.37392	1.37767	1.37851	1.38152	1.38297
$\partial n / \partial T$	0.00038	0.00037	0.00038	0.00039	0.00038	0.00040	-----

The crystal structure of acetic acid I was first reported by Jones and Templeton (19) who found it to be orthorhombic, space group $Pna2_1$, with the axes $a = 13.32 \pm 0.02$ Å, $b = 4.08 \pm 0.01$ Å and $c = 5.77 \pm 0.01$ Å, from single crystal X-ray diffraction measurements at 5°C . The structure consists of nearly planar, hydrogen-bonded, polymeric chains of acetic acid molecules, with the planes parallel to (100). These polymeric chains are stacked in layers along the a -axis with the long axes of the polymeric chains alternately being approximately parallel to (011) in one layer and (01 $\bar{1}$) in the other. The unit cell contains four molecules, two in each chain, with a resulting density of 1.27 g cm^{-3} . In 1970 this work was repeated by Nahrngbauer (18) and extended to include a structure determination at -190°C . The structure proposed by Jones and Templeton (19) at 5°C was confirmed and the axial lengths were reported, with increased precision, as $a = 13.310 \pm 0.001$, $b = 4.090 \pm 0.001$ and $c = 5.769 \pm 0.001$ Å and a resulting density of 1.270 g cm^{-3} . The structure at -190°C is the same as that at 5°C except for changes due to thermal expansion (18). The axial lengths at -190°C are $a = 13.214 \pm 0.001$, $b = 3.924 \pm 0.001$ and $c = 5.766 \pm 0.001$ Å with a density of 1.334 g cm^{-3} . These data show that the average volume expansivity of acetic acid I is 0.026 percent per Centigrade degree between -190°C and $+5^\circ\text{C}$ and that it occurs almost entirely

along the 'a' and 'b' axes. In addition, the molecular parameters and hydrogen bond lengths determined at -190°C and $+5^{\circ}\text{C}$ were almost identical indicating that the expansion is due to inter-chain expansion rather than expansion within each chain. These data also show that acetic acid II is not formed from acetic acid I when the sample is cooled to -190°C at atmospheric pressure. Neutron diffraction studies (27) of single crystals of acetic acid I at -150°C have located the hydrogen atoms and confirmed the structure determined by X-ray methods.

A variety of other physical measurements have been made on acetic acid, for example the viscosity (12, 28), surface tension (29), magnetic rotary power (30), specific magnetic susceptibility (31) and heat constants (3, 16, 32-37). Included in this were heat capacity measurements on the solid down to -185.7°C (33) but no evidence of a phase change was found.

1D. A Review of the Low Frequency Vibrational Spectra of Acetic Acid and Related Compounds.

The acetic acid monomer has C_s symmetry and 12 in-plane, A' vibrations and 6 out-of-plane, A'' vibrations. These vibrations can be approximately designated as 9 vibrations of the methyl group, 3 vibrations of the hydroxyl group and 6 vibrations of the heavy atom skeleton (38-40). None of these fundamental vibrations of the

monomer are below 400 cm^{-1} (38) even in perdeuterioacetic acid except for the internal rotation of the methyl group which has not been observed and is probably very weak (41).

Gaseous acetic acid dimers are known to be planar apart from the methyl hydrogen atoms, or extremely close to planar, from the electron diffraction measurements of Derissen (42). The molecular point group is taken to be C_{2h} . Those carboxylic acids which crystallize as dimers are also known to exhibit planar rings formed by the carboxyl group (43), so the usual assumption that acetic acid dimers are planar in the liquid is a reasonable one.

The dimer has 42 fundamental vibrations, 36 internal vibrations arising from the 18 vibrations of each monomer unit and 6 hydrogen-bond vibrations arising from the loss of six degrees of translational or rotational freedom when the two monomer molecules form a single dimer molecule. The 36 internal vibrations form the representation $12A_g + 6A_u + 6B_g + 12B_u$ under the point group C_{2h} ; where the $12A'$ vibrations of the monomer split into $12A_g$ and $12B_u$ vibrations in the dimer, and the $6A''$ vibrations of the monomer become $6B_g$ and $6A_u$ vibrations in the dimer. The gerade, g, and ungerade, u, vibrations are Raman and infrared active respectively. Thus each vibration of the monomer yields one infrared active and one Raman active vibration, whose frequencies differ by a small amount that is greater for the vibrations of the carboxyl

group than for those of the methyl group. The 36 internal vibrations have been studied for the gas and liquid phases, and are particularly well defined in a series of papers by Haurie and Novak (38, 44, 45). None of these vibrations absorb below about 400 cm^{-1} so they are not of further concern to the present work.

The six hydrogen-bond vibrations form the representation $2 A_g + 2 A_u + B_g + B_u$ under the point group C_{2h} ; the ungerade vibrations are again infrared active and the gerade vibrations are Raman active. These 6 vibrations must be discussed here because all of the interpretations in the literature of the far infrared spectrum of solid acetic acid are based on the dimer model rather than on the actual chain structure.

The forms of the six vibrations can be approximated by writing the six symmetry coordinates (46), based on the translational and rotational displacements of the two monomer units which do not correspond to overall translation or rotation of the dimer. These symmetry coordinates are depicted in Figure 1, numbered to correspond to those of Miyazawa and Pitzer (47). The actual B_u and B_g vibrations should correspond very closely to the symmetry coordinates S_3 and S_6 , respectively, because there are no other vibrations of like symmetry with similar frequencies. The two A_g vibrations are expected to correspond to linear combinations of S_1 and S_2 and the two A_u vibrations should

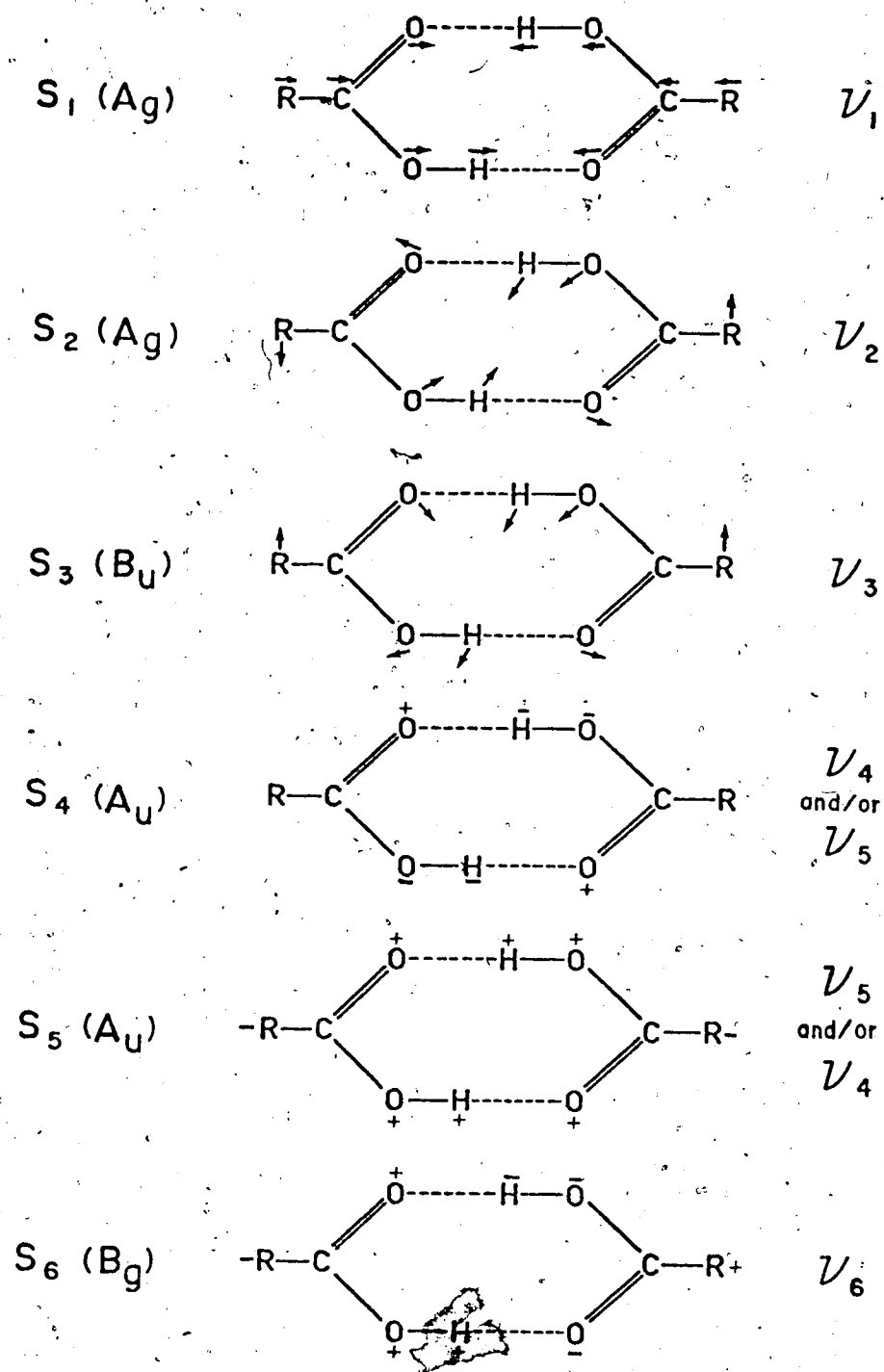


Figure 1. Symmetry coordinates (S_n) and vibrations (ν_n) of carboxylic acid dimers. For acetic acid, $R = \text{CH}_3$.

be linear combinations of S_4 and S_5 .

Miyazawa and Pitzer (47) calculated the frequencies of these vibrations using a rigid monomer model. The only far infrared frequency which they had as data for acetic acid was 188 cm^{-1} , which they attributed to Millikan and Pitzer (48) but which does not appear in that publication and, hence, is of uncertain origin. In order to obtain reasonable excess of data over adjustable force constants in the calculation, the entropy of dimerization was used and two simplifying assumptions were made: 1. that the force constants were the same for acetic and formic acids; and 2. that the bending force constants were the same for in-plane and out-of-plane motions. Three vibrational frequencies were available for formic acid dimer: 232 cm^{-1} (49), 237 and 160 cm^{-1} (48) so that, with assumption 1., sufficient data were available for the calculation. The calculation showed that ν_1 and ν_2 correspond to S_1 and S_2 , respectively but both ν_4 and ν_5 had nearly equal contributions from S_4 and S_5 . Table 4 gives the frequencies calculated for ν_1 to ν_6 .

Nakai and Hirota (50) observed a doublet absorption, with maxima at 188 and 167 cm^{-1} in the spectrum of gaseous acetic acid dimers. A similar doublet was seen (50) for $(\text{CD}_3\text{COQH})_2$, but for $(\text{CH}_3\text{COOD})_2$ they observed only a single absorption, with a questionable shoulder. Consequently they postulated that the doublet arose from proton tunnelling

Table 4. Low frequency vibrations observed and calculated for acetic acid dimer and its deuterated analogs. The physical state of the samples is indicated by g-gas, l-liquid, s-solution, m-matrix, and u-unstated. The reference is given at the head of each column of data.

Assignment (Figure 1)	Observed frequencies (cm ⁻¹) (CH ₃ COOH) ₂										
	(47) g	(50) g	(55) g	(56) g	(1) g	(51) l	(41) l	(58) l	(57) s	(62) m	(53) u
ν_1 (A _g)										162	
ν_2 (A _g)										65	
ν_3 (B _u)	188	{188 167}	190	{187 163}	{188 184(l) 176(s)}	{176 158 141}		177	182		
ν_4 (A _u)			168			75			87	80est.	
ν_5 (A _u)			50			40					
ν_6 (B _g)							{116 124(s)}		123	89	123
2 ν_1 (A _g)										310	
2 ν_2 (A _g)										120	
$\nu_5 + \nu_6$ (B _u)					168						
$\nu_4 + \nu_6$ (B _u)											168

Table 4. (continued)

Assignment (Figure 1)	$(\text{CD}_3\text{COOH})_2$		Observed frequencies (cm^{-1}) $(\text{CH}_3\text{COOD})_2$		$(\text{CD}_3\text{COOD})_2$	
	(50) g	(55) g	(50) g	(56) g	(52) 1	(41) 1
ν_1 (A_g)						
ν_2 (A_g)						
ν_3 (B_u)	{176 157}	180	{180 169(?)}	{183 161}	{176 164}	
ν_4 (A_u)		157				
ν_5 (A_u)		50				
ν_6 (B_g)						{106 115(s)}

Table 4. (continued)

Assignment (Figure 1)	(CH ₃ COOH) ₂			Calculated frequencies (cm ⁻¹) (CD ₃ COOH) ₂			(CH ₃ COOD) ₂			(CD ₃ COOD) ₂		
	(47)	(54)	(1)	(59)	(54)	(59)	(54)	(59)	(54)	(59)	(54)	(59)
ν_1 (A _g)	193	210		196	203	190	209	195	202	189		
ν_2 (A _g)	95	81		110	80	108 ^{exp}	79	108	78	106		
ν_3 (B _u)	180	187		180	179	167	184	178	176	166		
ν_4 (A _u)	80		79	67		58		65		57		
ν_5 (A _u)	46		54	47		43		47		43		
ν_6 (B _g)	128		130	115		109		113		108		

in a double-minimum potential for the displacement of the protons between the oxygen atoms. They assigned this absorption to $\nu_3(B_u)$ (Figure 1) and did not observe the bands due to the two A_u modes which are expected below 100 cm^{-1} .

In 1963 Stanevich (51) reported the spectrum of liquid acetic acid at 20°C from 250 to 140 cm^{-1} and from 120 to 10 cm^{-1} . His reported frequencies are listed in Table 4. Three features were reported between 180 and 140 cm^{-1} , all of which were assigned to $\nu_3(B_u)$ (Figure 1), the asymmetric stretch of the hydrogen bonds. Stanevich assigned two of the three features to hot bands of the ν_3 vibration. Two other broad absorptions centered at 75 and 40 cm^{-1} were reported for the first time and were assigned to ν_4 and ν_5 respectively (Figure 1, Table 4) on the basis of Miyazawa and Pitzer's calculations (47). The following year Stanevich (52) reported the spectrum of liquid $(\text{CH}_3\text{COOD})_2$ from about 210 to 140 cm^{-1} and 120 to 30 cm^{-1} and that of liquid $(\text{CD}_3\text{COOD})_2$ from 200 to 140 cm^{-1} and 120 to 80 cm^{-1} . The assignment of these spectra followed that of $(\text{CH}_3\text{COOH})_2$ and the observed frequencies with their assignments are shown in Table 4.

In 1964 Zirnit and Sushchinskii (53) reported the Raman spectrum of liquid acetic acid below 250 cm^{-1} . They did not specify the temperature or the lowest frequency which they could reliably observe but they did report a line at 123 cm^{-1} which they assigned to the B_g out-of-plane symmetric deformation vibration, ν_6 , on the basis of the calculations done by Miyazawa and Pitzer (47).

The discovery of this line adds significant support to the validity of these calculations.

Also in 1964, Kishida and Nakamoto (54) published a normal coordinate calculation of the in-plane vibration of acetic acid dimer. They were mainly concerned with the internal vibrations of the monomer units and their data for the vibrations involving the hydrogen bonds consisted of the frequencies calculated by Miyazawa and Pitzer (47) plus the one experimental frequency available to them (47). As a result the main value of their calculations is that the vibrational frequencies were also predicted for the deuterated species $(CD_3COOH)_2$ at room temperature, between 400 and 33 cm^{-1} . Their calculated frequencies are shown in Table 4.

In 1965 Carlson, Witkowski and Fateley (55) published infrared spectra of gaseous $(CH_3COOH)_2$ and $(CD_3COOH)_2$ at room temperature, between 400 and 33 cm^{-1} . Their observed frequencies are shown on Table 4. Of the four frequencies reported for $(CH_3COOH)_2$, the absorption at 310 cm^{-1} was neither assigned nor even discussed. The 50 cm^{-1} absorption was assigned to $\nu_5(A_u)$, the out-of-plane hydrogen bond bend, and the 190 cm^{-1} absorption was assigned to $\nu_3(B_u)$, the asymmetric hydrogen bond stretch; by direct comparison with the calculated frequencies of Miyazawa and Pitzer(47). The feature at 168 cm^{-1} was assigned to $\nu_4(A_u)$ (Figure 1) even though

the possibility of a combination band of $\nu_5 + \nu_6$ in Fermi resonance with ν_3 and the possibility of proton tunnelling were considered. In contrast to previous workers these authors equated ν_4 with S_4 and ν_5 with S_5 (Figure 1) for reasons that were not stated.

In 1967 Ginn and Wood (56) showed that the doublet at $190/168 \text{ cm}^{-1}$ in $(\text{CH}_3\text{COOH})_2$ is almost certainly not due to proton tunnelling, because a corresponding doublet at $183/161 \text{ cm}^{-1}$ was observed in $(\text{CH}_3\text{COOD})_2$. They attributed the doublet to a combination of the effects of Fermi resonance between ν_3 and $\nu_5 + \nu_6$ and of the rotational band contours.

Between mid 1967 and mid 1968 four papers reported low-frequency spectra of dimeric acetic acid in the liquid phase or in solution in various solvents. Fauquembergue, Constant and Raczy (57) reported a strong absorption centered at 182 cm^{-1} , a weak absorption at 123 cm^{-1} and a broad, but fairly strong, absorption centered around 87 cm^{-1} by CH_3COOH in 5% solution in benzene and in carbon tetrachloride. No assignment was discussed other than that these frequencies had been calculated by Miyazawa and Pitzer (47). Waldstein and Blatz (41) reported low frequency Raman spectra of liquid $(\text{CH}_3\text{COOH})_2$ and $(\text{CD}_3\text{COOD})_2$ and solutions of these acids in n-pentane and water at 25°C . They observed a line at $116 \pm 5 \text{ cm}^{-1}$ for the pure liquid, and a line at $124 \pm 5 \text{ cm}^{-1}$ for the n-pentane solution of $(\text{CH}_3\text{COOH})_2$, which they assigned to the ν_6 fundamental (Figure 1) predicted by Miyazawa

and Pitzer(47) to be at 128 cm^{-1} . The comparable lines for $(\text{CD}_3\text{COOD})_2$ were at $106\pm 5\text{ cm}^{-1}$ and $115\pm 5\text{ cm}^{-1}$ respectively. Another line, at $47\pm 7\text{ cm}^{-1}$ in the spectrum of $(\text{CH}_3\text{COOH})_2$ in the pure liquid and in solution was called a "liquid structure" line and a third line, possibly present at 95 cm^{-1} in the liquid, was assigned to open dimers or polymers. Saunders, Bentley and Katon (58) reported a broad absorption, centered at 177 cm^{-1} , by $(\text{CH}_3\text{COOH})_2$ in the liquid phase and in benzene solution, presumably at room temperature.

The last of the four papers is by Jakobsen, Mikawa and Brasch (1) and presents the infrared spectra between 300 and 50 cm^{-1} of acetic acid dimer in the gas, liquid and hexane solution states. In the corresponding spectra they observed absorption bands at 188 cm^{-1} , 184 cm^{-1} and 176 cm^{-1} respectively, and assigned them to ν_3 , the asymmetric hydrogen bond stretching vibration (Figure 1). For the vapor they also observed an absorption at 168 cm^{-1} and assigned it to $\nu_5+\nu_6$ in Fermi resonance with ν_3 . This assignment was based on their normal coordinate calculations for the out-of-plane vibrations of the dimer, and on their observed frequency difference between the ν_4 vibrations of $(\text{HCOOH})_2$ and $(\text{DCOOH})_2$, from which they excluded ν_4 as a possible assignment of the 168 cm^{-1} absorption in $(\text{CH}_3\text{COOH})_2$. The force constants used were taken from a similar

calculation on formic acid dimer, in which the force constants were determined from their experimental data on $(\text{HCOOH})_2$ and confirmed by correctly giving the frequency of ν_4 of $(\text{DCOOH})_2$. The out-of-plane, symmetric, hydrogen bond bending vibration (ν_6 in Figure 1) was listed as having B_u symmetry under point group C_{2h} but it is assumed that this was meant to be B_g . Their calculated and observed frequencies, with assignments, are listed in Table 4.

In 1969 Fukushima and Zwolinski (59) presented a normal coordinate calculation for $(\text{CH}_3\text{COOH})_2$, $(\text{CH}_3\text{COOD})_2$, $(\text{CD}_3\text{COOH})_2$ and $(\text{CD}_3\text{COOD})_2$. They were mainly interested in the internal vibrations of the monomer units and their data for the region below 400 cm^{-1} were primarily the frequencies calculated by Miyazawa and Pitzer (47). As a result the main value of this work to the present discussion is that they predicted the frequency shifts due to deuteration of the acetic acid dimer. Their calculated frequencies are presented in Table 4.

Recently, Witkowski (60) has proposed a new interpretation of the doublet absorption between 150 and 200 cm^{-1} by acetic acid dimers. He appears to argue that the A_g hydrogen bond stretching vibration, ν_1 of Figure 1, becomes infrared-active as a result of coupling with the OH stretching modes. As a result the absorptions observed at 190 and 168 cm^{-1} by Carlson *et. al.* (55) are assigned to ν_3 and ν_4 , respectively, by Witkowski. This work

stems from Witkowski's previous interpretation of the OH stretching region of the spectrum, based on his theory (61) which presents a model for strong coupling between the O-H and O...O stretching modes. There is evidence (44) that at least some of the assignments of the bands in the OH stretching region which result from this model are not correct.

A quite different assignment of the low-frequency vibrations of acetic acid dimer was published in 1971 by Redington and Lin (62). These authors studied the infrared spectrum of the OH stretching region of acetic acid dimers matrix isolated in Argon at 4°K, and assigned the observed features as combination transitions of the OH stretching fundamental and of the overtone of the in-plane C-O-H deformation with low-frequency vibrations. They used the low-frequencies deduced from these combination bands with the experimental infrared data obtained from the gas by Carlson *et. al.* (55) to make the assignment shown in Table 4. The arguments presented in support of their assignment were not particularly self-consistent or clearly presented. Furthermore, Grenie, Cornut and Lassegues (63) have recently shown that Redington and Lin's (62) assignment of the mid-infrared bands are not consistent with the isotope shifts observed when $\text{CH}_3\text{C}^{18}\text{O}^{18}\text{OH}$ is used instead of the normal species, although

no alternative assignment was presented for some of the bands. Therefore it is concluded that Redington and Lin's assignment is possible but is not clearly an improvement over earlier assignments.

It can be seen from the above discussion and the frequencies summarized in Table 4 that, while a large number of reports on the low-frequency spectra of the dimeric acid have been published, our present knowledge of the hydrogen-bond vibrations leaves much to be desired.

In solid acetic acid I, two different chains contribute two monomer molecules each to the unit cell (18, 19, 27) (Section 1C). The space group is $Pna2_1-C_{2v}^9$ (19) which shows that the unit cell group (64) is isomorphous with the point group C_{2v} . To a first approximation, the only vibrations in an ordered solid which can be infrared or Raman active are those in which the atomic displacements in one unit cell are simultaneously reproduced in all other unit cells (65). These vibrations are called zero-wave-vector vibrations. Thus, to determine the infrared or Raman activity it is only necessary to consider the vibrations within one unit cell, under the symmetry of the unit cell group.

There are four vibrations in each unit cell for each internal degree of freedom of each monomer unit. These four vibrations form a regular representation (66) under the unit cell group, and three of them are infrared-

active and all four are Raman-active. Haurie and Novak (67) have studied and assigned the infrared spectrum of the internal vibrations of the monomer units in acetic acid I. They observed the spectrum from 4000 to 400 cm^{-1} at 0°C and -180°C and found they could interpret their data by considering only a single chain. The interactions between molecules in the chain are, therefore, much stronger than the Van der Waals interactions between the chains, as is expected. The unit cell group of each isolated infinite chain is isomorphous with the point group C_s and the repeating unit of the chain contains two acetic acid molecules; thus all the vibrations are infrared active and two rather than three components are observed in the infrared spectrum from each internal monomer vibration. However, there are no absorptions due to these vibrations below about 400 cm^{-1} , so they will not be further discussed here.

Even though the crystal structure of acetic acid I was known to consist of polymeric chains before the far infrared spectrum was observed, all of the literature interpretations of the far-infrared spectrum of the solid are based on a dimer model. As a result a theoretical discussion of the inter-monomer hydrogen bond vibrations of acetic acid I is not needed here and will be left until Chapter 5.

The far infrared spectrum of solid acetic acid was

first published in 1963 by Stanevich (51), who observed the spectrum at -175°C between 250 and 140 cm^{-1} and between 120 and 30 cm^{-1} . He observed absorption bands at 232 , 196 , 83 and 42 cm^{-1} and assigned them on the basis of the calculations done by Miyazawa and Pitzer (47), using the notation shown in Figure 1. The 196 , 83 and 42 cm^{-1} absorptions were assigned to ν_3 , ν_4 , and ν_5 , respectively and the 232 cm^{-1} absorption was attributed to an internal vibration of the carboxyl group because there were no hydrogen bond vibrations expected at this frequency and because he had observed similar absorptions in other carboxylic acids.

The following year Stanevich (52) reported the infrared spectra of CD_3COOD and CH_3COOD at -175°C in the same frequency regions as he used previously for CH_3COOH (51). For CH_3COOD he observed absorption bands at ~ 232 , 195 , 82 , and 43 cm^{-1} and assigned them, as before (51), to COOH , ν_3 , ν_4 , and ν_5 , respectively. For CD_3COOD he observed bands at 190 , 78 and 42 cm^{-1} and assigned them to ν_3 , ν_4 , ν_5 respectively; his reported spectrum stops at 220 cm^{-1} so one does not know if an absorption was present near 230 cm^{-1} as was found for the other acids.

Carlson, Witkowski and Fateley (55), in 1965, reported the far infrared spectrum of acetic acid at liquid nitrogen temperature between 400 and 33 cm^{-1} but they only observed a single intense absorption at 198 cm^{-1} , which

they did not assign. They were aware of the data reported by Stanevich (51) but were unable to observe any evidence of the 83 and 42 cm^{-1} bands, even with very thick samples.

The most recent paper on the low-frequency spectrum of solid acetic acid was published in 1967 by Jakobsen, Mikawa and Brasch (1), who reported the spectrum at about -150°C between 370 and 60 cm^{-1} . They were aware of the polymorphism present in acetic acid, but were unsure which polymorph corresponded to their reported spectrum. However, since their sample was formed by freezing the liquid, it is assumed that they had acetic acid I. The vibrational frequencies they observed were 198, 126 and 82 cm^{-1} . Jakobsen et. al. (1) stated that they interpreted their data on the basis of a polymeric chain structure having C_s symmetry and hence expected 8 infrared-active vibrations, but the actual assignments that they gave correspond to those of the dimer configuration. They assigned the 198 cm^{-1} band to the hydrogen bond stretching vibration, ν_6 , and, tentatively, the 82 cm^{-1} band to the twisting mode, ν_5 (Figure 1). They did not discuss how they transposed the dimer vibrations to apply to the polymers. Since this is the most recent investigation of the low frequency vibrations of solid acetic acid, it leaves the spectrum and its assignment very much uncertain.

The low frequency spectrum of solid propionic acid is of interest for comparison with that of acetic acid. In the solid phase propionic acid consists of

centrosymmetric cyclic dimers, crystallized in the space group $P2_1/c-C_{2h}^5$ with four monomers per unit cell (68).

As a result, since each monomer of propionic acid contains eleven atoms, there are 27 internal vibrations per monomer and a total of 108 internal vibrations per unit cell.

These internal vibrations are not of particular interest here and will not be discussed in detail, but some of them do appear in the region below 400 cm^{-1} . There are also twenty-four lattice, or inter-monomer, vibrations expected; of which three are simple translations of the whole unit cell and have zero frequency. The remaining twenty-one rotational and translational lattice vibrations, several of which involve bending and stretching of the hydrogen bond, are the primary concern here, and are listed in Table 5.

Stanevich (51), in 1963, was the first to report the far infrared spectrum of solid propionic acid. He reported the spectrum at -175°C between 250 and 30 cm^{-1} , and observed absorption bands at 229 , 176 , 126 , 78 and 40 cm^{-1} , which he assigned, by comparison with acetic acid, to a carboxyl group internal vibration, ν_3 (Figure 1), an alkyl group internal vibration, ν_4 , and ν_5 , respectively (Table 6).

In 1969 Jakobsen, Mikawa and Brasch published two papers (69, 70) which reported the far infrared spectrum of solid propionic acid. In the first (69), the spectrum

Table 5. Lattice Vibrations of Propionic Acid

Description	Symmetry under the unit cell group, isomorphous with C_{2h}	
	I R	R
Translation of the dimer along the x-axis	A_u	
Translation of the dimer along the y-axis	B_u	
Translation of the dimer along the z-axis	A_u	
Hydrogen bond stretch (ν_3) ^a	A_u, B_u	
Out-of-plane bend (ν_4) ^a	A_u, B_u	
Twist, ring deformation (ν_5) ^a	A_u, B_u	
Hydrogen bond stretch (ν_1) ^a		A_g, B_g
Rotation in-plane of the dimer unit		A_g, B_g
Rotation out-of-plane of the dimer unit		A_g, B_g
Rotation out-of-plane of the dimer unit		A_g, B_g
Bend in-plane (ν_2) ^a		A_g, B_g
Bend out-of-plane (ν_6) ^a		A_g, B_g

a. See Figure 1

was recorded at -150°C between 250 and 60 cm^{-1} , using either a film of propionic acid solidified between two polyethylene plates or a sample absorbed into a polyethylene film. In the second paper (70), the spectrum of a polycrystalline sample at liquid nitrogen temperature was recorded between 300 and 50 cm^{-1} , but the spectrum was only shown between about 200 and 60 cm^{-1} . They also reported the spectrum of $\text{CD}_3\text{CD}_2\text{COOD}$ using the same procedure, and all their observed frequencies and assignments are listed in Table 6. They considered that the intermolecular vibrational coupling is so weak that the crystal vibrations of different symmetry which result from the same dimer vibration are unresolved, so they assigned the observed bands to vibrations of a single dimer. These assignments were made on the basis of comparisons with those of formic and acetic acids, deuteration shifts, and a normal coordinate calculation. The force constants for the normal coordinate calculation were those used for acetic and formic acids (1), except that an additional force constant for the torsion about the C-C bond was required and was estimated simply by choosing a value slightly less than the force constant for the torsion about the C-O bond.

The main disagreement between this and Stanevich's assignment (51) concerns the 226 , 78 and 40 cm^{-1} absorptions. The 226 cm^{-1} band was considered to be due to ice condensing on the outside of the cell during the

Table 6. Observed Frequencies and Assignments for $\text{CH}_3\text{CH}_2\text{COOH}$ and $\text{CD}_3\text{CD}_2\text{COOD}$ solids in the low-frequency region. The reference is given at the head of each column of data.

Observed Frequencies (cm^{-1})				Assignments	
$\text{CH}_3\text{CH}_2\text{COOH}$		$\text{CD}_3\text{CD}_2\text{COOD}$			
(51)	(69) ^a	(69) ^b	(70) (71)	(70)	(51) (69, 70) (71)
229	226	226		317	
176	169	160	169	150	ν_3^c H-bond stretch, ν_3^c
126	121	132	121	100	R group C-C Torsion
78	77	78	77	74	ν_4^c twist (ring) ν_5^c
40					ν_5^c H-bond bend ν_4^c
				109	Bend out-of-plane ν_6^c
				81	Rotation out-of-plane
				71	Bend in-plane ν_2^c
				55	Rotation out-of-plane or Rotation in-plane

^a film between polyethylene plates

^b sample absorbed into a polyethylene film

^c see Figure 1.

cooling process, because they did not predict any vibrations to be at that frequency and because they noticed an increase in intensity with longer cooling times. The assignments for the 78 and 40 cm^{-1} bands were reversed from Stanevich's assignment (51) on the basis of their normal coordinate calculations.

In 1971 Jakobsen, Mikawa, Allkins and Carlson (71) published the low-frequency Raman spectrum of polycrystalline propionic acid at 135°K in a liquid-nitrogen cooled cell. Four bands were observed: a strong band at 71 cm^{-1} and three weaker bands at 109, 81 and 55 cm^{-1} .

A tentative assignment, shown in Table 6, was based on their normal coordinate calculations (70) and on comparisons with the assignments for formic and acetic acids. The assignment for the 55 cm^{-1} band was left open to debate, but they did say that it was due to either an in-plane or an out-plane rotational vibration.

1E. Objectives of this work

In general terms the primary aim of this work is to obtain data on the physical properties of acetic acid II, in order to characterize it and its phase diagram below 0°C. All of the available evidence indicates that acetic acid I does not change to acetic acid II when it is cooled at one atmosphere pressure. On the other hand, though, an extrapolation of Tammann's (2) and Bridgman's (3) acetic acid I to II equilibrium line indicates that the one

atmosphere phase transition should occur at $-56 \pm 3^\circ\text{C}$, and Tammann (2) did report having observed a phase transition at -71.0°C and 1 Kg cm^{-2} pressure. Jakobsen, Mikawa and Brasch (1) observed two phases using a diamond, high-pressure apparatus but found only one of the phases by cooling a sample of acetic acid. Nahringsbauer (18) stated that he is seeking the second polymorph of acetic acid for X-ray study but neither he nor Jakobsen et. al. (1) appeared to be aware of the work done by Tammann (2) and Bridgman (3).

Therefore the objectives of this work are as follows:

(i) To map out the phase diagram for the solid-solid phase transition of acetic acid to see whether phase II can be formed at one atmosphere and to see at what temperatures it is stable at one atmosphere.

(ii) To record the X-ray powder diffraction pattern of acetic acid II, to characterize the phase and, if possible, to deduce the crystal symmetry and the unit cell dimensions.

(iii) To record the far infrared spectrum of acetic acid II, in order to obtain evidence concerning the difference between phases I and II. The spectra of acetic acid I and propionic acid at liquid nitrogen temperature were redetermined using the techniques used for acetic acid II, in order to compare them with the spectrum of acetic acid II, to help in its assignment.

Chapter 2. Experimental

2A. Purification of Chemicals

Glacial acetic acid with a stated purity of 99.8% was obtained from Canadian Industries Limited. The main impurity expected was water, and samples from freshly opened bottles were analyzed for water by Karl Fischer titrations (72, 73). The Karl Fischer reagent was calibrated by determining the titre required for 10 μ l of water before and after the titration of the sample, which was found to contain 0.11% of water, well within the purity limit claimed.

The measurements of the phase diagram of acetic acid are very sensitive to the presence of water (74, 75). The samples used for such measurements were, therefore, further purified by zone-refining (76). Glass zone-refining tubes, 6 mm inside and 8 mm outside diameter and 12-14 inches long, were used. About 8 ml of acetic acid from a freshly-opened bottle was placed into the tube which was then sealed. The purification process was begun by cooling the tubes containing the acetic acid samples and mounting them in the zone refiner. With care liquid acetic acid can easily be super-cooled down to 5°C, which makes it very convenient to directionally freeze the sample by using the zone refiner to raise the tube past the heater at the rate of $\frac{1}{2}$ inch per hour. A seed crystal was produced at the top of the sample tube by cooling a

small area of glass with dry ice and the heater prevented the whole sample from solidifying at once. As a result the acetic acid above the heater was crystalline and that below the heater was super-cooled liquid, so that the directional freezing was controlled by the 0.5 inch per hour rate at which the tube was raised past the heater. The zone-refining apparatus was designed and constructed in this department to fit into a refrigerator, so that the ambient temperature could be kept at about 5°C. The zone-refining process involved drawing the tubes vertically through a heater which created a liquid zone which moved down the tube at a rate of 0.5 inch per hour. The zone lengths were controlled to 1 inch, and each sample was passed through the heater in this way at least fourteen times. When the zone refining was complete the bottom 20% of the sample always appeared white and polycrystalline whereas the top 80% appeared almost clear. The top 60% of the zone-refined sample was used for experiments on the phase diagram. The sealed tubes of zone-refined acetic acid were kept at 5°C and were used within a few days after the zone-refining process was completed.

In order to be absolutely sure of the water content of a typical sample used for the phase diagram study, one sample was treated in the following way. A sample of zone-refined acetic acid was placed in the high pressure cell and kept there for four days. During the four days,

3 experiments were carried out to measure the pressure required for the phase transition to occur at 0°C.

After the four days the pressure was released and the cell was warmed up to melt the acetic acid. A sample was removed in a syringe and a Karl Fischer titration was carried out on this recovered sample. One drop of titrant was sufficient to complete the titration, indicating that the sample still contained at most 0.015% of water.

Propionic acid was obtained from Fisher Scientific Company. The manufacturer's specifications showed only 0.05% water, and a boiling range of 140.6-141.4°C. Since the propionic acid was used only for the study of its infrared spectrum, and not for phase diagram measurements, the purity of the manufactured product was assumed to be adequate. However only propionic acid taken from a freshly opened bottle was used.

The water used for calibration of the pressure gauges was triply distilled, once from permanganate and twice from glass. Once converted to ice, it was also taken through the ice I to ice III phase transition several times, because this has been shown to result in further purification (77, 78). However it was subsequently found that water which was simply distilled and freshly boiled to remove gaseous contamination gave the same results.

2B. Apparatus and Sample Handling Methods for the Phase Diagram Measurements

The high pressure apparatus shown in Figure 2 was a steel cylinder (B) having an inside diameter of 1.0015 inches and an outside diameter of approximately 5 inches. The cylinder was fitted with pistons (A), 1.000 inch in diameter, at each end whereby the pressure could be applied. The pistons were made of Vascomax 350 and the cylinder of Vascomax 300, 18% nickel maraging steels, which were subsequently heat treated to about 50 Rockwell C. Sample extrusion around the pistons was prevented by two brass back-up rings (E) which had a triangular cross-section and which provided a perfect seal between the pistons and the cylinder for solid samples.

The pistons and cylinder were mounted inside a cooling jacket (F) which allowed liquid coolant to circulate around the cell but did not allow the coolant to come into contact with the piston-cylinder junctions. This cooling jacket provided an easy means of controlling the temperature within the cell at high pressure, and allowed the cell to be cooled to the desired temperature (say -15°C) before the sample (C) was introduced. This procedure of precooling the cell made it possible to inject liquid acetic acid into the cell where it immediately froze. One problem that arises from this procedure is that water tends to condense into the cell while it is

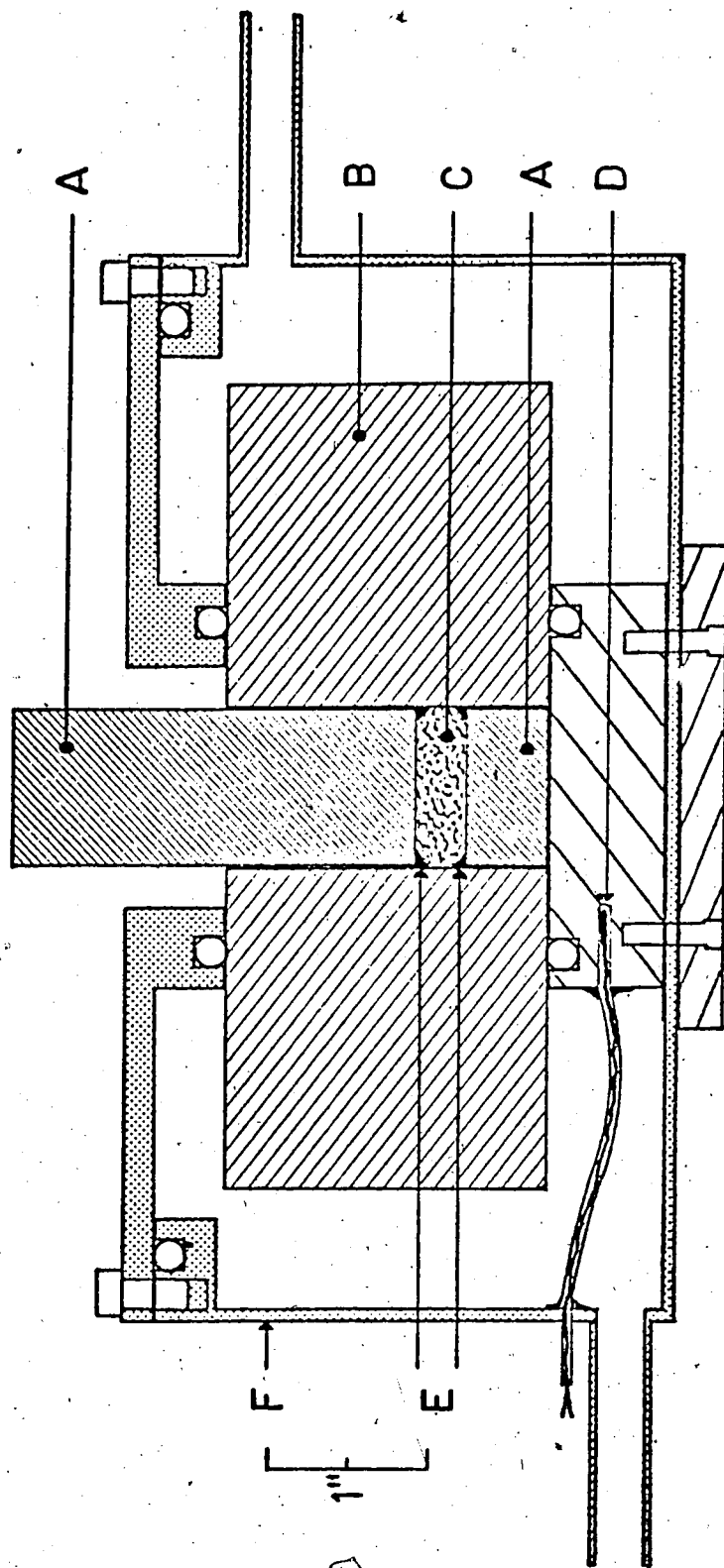


Figure 2. The high pressure cell used for the phase diagram studies. The lettered parts of the cell are as follows: A - the pistons, B - the cylinder, C - the sample, D - the thermocouple, E - the back-up rings and F - the coolant jacket.

being precooled. In order to overcome this problem, the top of the assembly was covered by a clear plastic sheet and dry nitrogen gas was blown into the cell. This kept a dry atmosphere around the top of, and within, the cell.

The acetic acid samples were transferred from the zone-refining tubes to the pressure cell in the following way, using a dry box filled with nitrogen gas which had been dried by three, 12 inch columns of molecular sieve and which was kept dry by phosphorous pentoxide inside the box. The zone-refining tube containing the acetic acid sample was cooled to 77°K by immersion in liquid nitrogen, then removed from the liquid nitrogen and very quickly placed in the entrance chamber of the dry box. Insulation was provided for the tube in the entrance chamber so that the sample would not melt while the chamber was being evacuated and refilled with dry nitrogen gas. As soon as the entrance chamber had been filled with dry nitrogen the cold tube and sample were transferred into the dry box and the tube was broken open such that the bottom 40% of the sample could be discarded into a beaker and the top 60% of the sample could be melted out of the tube into a 50 ml round bottom flask. The whole process from immersion in liquid nitrogen till the tube was broken open took between 5 and 6 minutes and no melting of the sample was ever observed during that time. The acetic acid was

allowed to melt in the round bottom flask until only a small amount of solid remained. At this point a 4 ml sample was taken in a 5 ml syringe. The syringe and its contents were placed inside a plastic bag, removed from the dry box, and taken three or four feet to the precooled pressure vessel. The needle of the syringe was poked through the plastic and into the cell, the sample was injected into the cell where it froze immediately, and the piston was put into the cell. After the sample was allowed to thoroughly cool and solidify for a few minutes, the pressure was applied to compact the sample. Once the pressure within the cell reached 250 bars it was assumed that no contamination from the atmosphere could occur, and the flow of nitrogen gas over the surface of the assembly was shut off. If at a later time the pressure needed to be lowered below 250 bars then the dry nitrogen gas flow was always restarted, as a precaution.

The syringe, round bottom flask and beaker were dried in an oven at 150°C for many hours before placing them, still hot, into the dry box. Before being dried in this way, the syringe was calibrated using water at its melting point as a standard and the volume of acetic acid used is believed to be known to $\pm 0.1 \text{ cm}^3$. From the density (32) and volume, the weight of acetic acid used for each experiment was calculated.

The pressure was produced by a 20 ton press of

standard design, equipped with an O-ring oil seal on the ram instead of the usual leather skirt. The pressure within the cell was determined by the square of the ratio of the radius of the high pressure cylinder (diameter = 1.0015 inches) to the radius of the ram in the press (diameter = 2.625 inches). The oil pressure was measured on two, factory-calibrated, 1 1/4 inch Heise Bourdon gauges. One gauge covered the range 0 to 500 bars and the other 0 to 100 bars with stated accuracies of 0.5 and 0.1 bar, respectively. Both gauges were zeroed before a run and checked again after a run. The pressure calibration of the whole assembly was checked by measuring the ice I-III equilibrium pressure at -25°C and comparing the result with that obtained by Kell and Whalley (79). Kell and Whalley reported an equilibrium pressure of 2098 bars at -25°C which agrees to within 4 bars with the results obtained here. This agreement is very slightly poorer than that expected from the accuracy of the gauges.

Volume changes were determined from measurements of the distance between the plattens of the press. Two Starrett dial gauges (#656-617, smallest division 10^{-4} inch) were accurately set diagonally across from each other at the corners of the plattens, equidistant from the center. The average of the reading of the two gauges was used to determine the change, Δl , in the separation of the plattens, and the volume change, ΔV , was calculated.

Using the equation: $\Delta V = \pi r^2 \Delta l$, where r is the radius of the pressure cylinder at atmospheric pressure. The volume changes calculated in this way do not distinguish between the true changes in the sample volume and changes in the separation of the plattens due to the compressibility in the apparatus. However, the volume change at the phase transition was measured at a constant pressure, so it is not affected by the compression of the apparatus.

Temperature control was achieved by circulating methanol, from a Neslab LT9 low-temperature thermostat bath, through the cooling jacket surrounding the cell, by means of the circulating pump on the thermostat bath. The hoses through which the methanol flowed were insulated and the cooling jacket around the cell was also insulated. The temperature of the cell was measured by a copper-constantan thermocouple, with the reference junction at 0°C in an ice-water slurry. A Honeywell model 2733 slide-wire potentiometer was used to measure the thermocouple voltage and hence the temperature. The temperature measurement was calibrated with several constant temperature baths from +100°C to -80°C. A Hewlett-Packard 2801A quartz crystal thermometer which had been calibrated against an NBS platinum resistance thermometer was used as the standard. The thermocouple voltages above and below 0°C were fitted to separate quadratic functions of temperature, using the least squares technique, and voltages were calculated at 1 degree intervals from -150

to 0°C and from 0 to 150°C and arranged in a table. Temperatures were then determined from the thermocouple voltages by interpolation between the points in the table and they agreed to within 0.1°C with those given by the Hewlett Packard quartz crystal thermometer. The thermocouple was placed in the base of the cell, in a small hole which was drilled into the steel block as shown in Figure 2. The hole was then sealed around the thermocouple wire in order to prevent coolant liquid from coming in contact with the thermocouple. The temperatures reported are believed to be those of the sample to within 0.5°C and were constant to within 0.1°C for the time during which measurements were made.

2C. Preparation of Acetic Acid II and Ground Samples

Acetic acid II at 1 atmosphere and 77°K was required for the X-ray and spectroscopic studies, and was prepared in the following way. Glacial acetic acid, 99.8% pure was loaded into a piston-cylinder high pressure cell and pressurized, using the techniques described in Section 2B. The high pressure cell was identical to that described in Section 2B, except that the lower half of the bore was conically tapered so that the diameter at the bottom of the cylinder was 0.010 inches greater than that half-way up the bore. This taper facilitated the removal of the sample from the cell. The cell sat in a metal cup, as shown in Figure 3a, and was kept at about -10±10°C by pouring small quantities

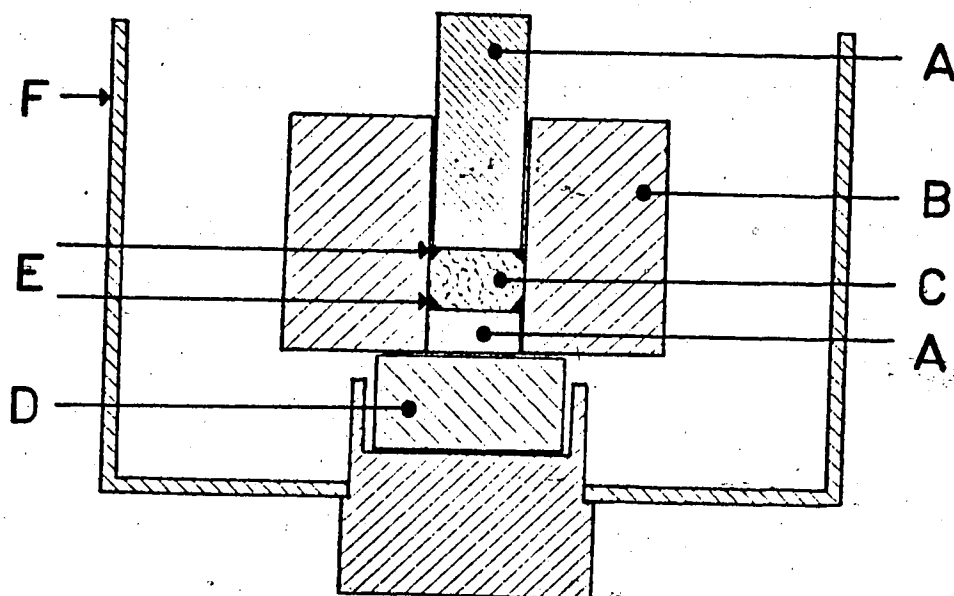


Figure 3a

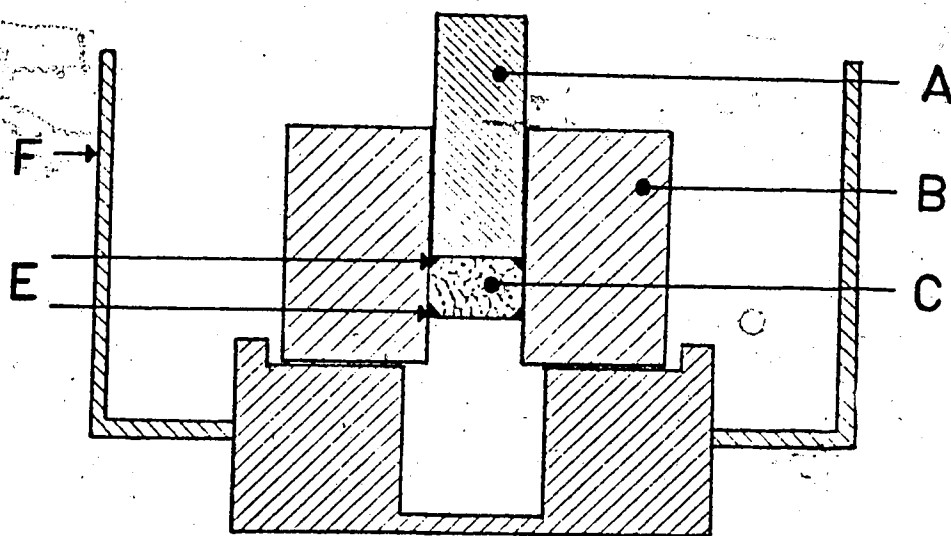


Figure 3b

Figure 3. The high pressure cell used to prepare (Figure 3a) and recover (Figure 3b) acetic acid II. The lettered parts of the cell are as follows: A - the pistons, B - the cylinder, C - the sample, D - hardened steel block, E - the back-up rings and F - the metal cup.

of liquid nitrogen into the cup from time to time. The pressure was increased to 2500 bars and left for one hour to ensure that the acetic acid was totally transformed to phase II. Liquid nitrogen was then poured into the cup and when the pressure cell had been cooled to 77°K, the pressure was released to atmospheric pressure. The pressure cell was then transferred quickly to the cup shown in Figure 3b, which contained liquid nitrogen, and pressure was again applied to force the sample out of the cell into the cup. The sample was then placed into a screw-topped, glass vial, which was placed inside a similar vial and stored under liquid nitrogen until required.

Samples of acetic acid II, acetic acid I and propionic acid were ground to a fine powder for X-ray and spectroscopic study. The samples were powdered at liquid nitrogen temperature, either by a Spex, Freezer-Mill, power grinder or by hand-grinding with a mortar and pestle. It was found that the rapid cooling of the sample to 77°K, in the pressure vessel for acetic acid II or in a mortar for acetic acid I, usually caused the resulting crystals to be extremely small. Little grinding was then necessary to convert the solid obtained to a fine powder. In the grinding process it was necessary to take precautions against heating the sample. This was especially true with the power grinder when acetic acid II was being ground, since the sample could transform back to acetic acid I if the temperature increased to above about -60°C. In order to prevent the temperature from increasing significantly,

the grinding was done in periods of 10 to 30 seconds with one or two minutes cooling time between the grinding periods. When the grinding was complete, the powdered sample was placed in a vial inside a second vial and was stored under liquid nitrogen until required.

All manipulation of acetic acid II, powdered acetic acid I and powdered propionic acid was carried out on a table in an uninsulated can containing liquid nitrogen using long tweezers and spatulas. These techniques are described more fully in Section 2E.

2D. X-Ray Experimental and Method

The X-radiation was produced by an Enraf-Nonius "Diffractis 601" generator. Copper, cobalt or chromium targets were used, and the radiation was filtered by sheets of nickel, iron or vanadium pentoxide respectively to remove white and β radiation (80, 81). The resulting $K\alpha$ radiation had wavelengths of 1.5418 Å for copper, 1.7902 Å for cobalt and 2.2909 Å for chromium (80). A Jarrel-Ash precession camera was used as a flat-plate powder camera. The X-ray film was obtained from Ilford Ltd. of England and was of Industrial G quality. The sample to film distance was 60.0 mm and was calibrated using sodium chloride powder as a standard at 295°K (82) and ice Ih at 120°K (83). The samples were contained in quartz

capillaries with an internal diameter of 0.5 or 0.3 mm and a wall thickness of 0.01 mm. The capillaries were mounted on the goniometer head via a bakelite adapter designed to shield the metal goniometer head from the cold nitrogen stream, which was used to cool the sample.

The samples were prepared as described in Section 2C, and all operations required to place the sample into a capillary and mount it on the goniometer head were carried out in a can containing boiling liquid nitrogen, as described in Section 2E. In order to fill a capillary, it was placed in a hole in a brass block and cooled. The powder was then carefully transferred, a few granules at a time, into the capillary. Long metal spatulas were used to transfer the powder and very thin glass rods were used to pack the sample firmly into the capillary. The capillary was then mounted in the bakelite adapter on the goniometer head and carried to the X-ray camera. The capillary was immersed in liquid nitrogen while being carried to the camera, and as soon as it was mounted on the camera it was kept cold by a flow of cold nitrogen gas. This flow of coolant gas was maintained continuously and was begun at least one half hour before the capillary was mounted in place. The coolant gas was produced by boiling liquid nitrogen and conducting the cold gas through a glass dewar tube to the sample site. To prevent condensation of water onto the cold capillary, a continuous stream of

warm, dry nitrogen gas surrounded the cold stream and flowed coaxial to it. In this way the sample could be maintained between room temperature and 100°K for periods of up to 24 hours.

The sample temperature was measured by placing an iron-constantan thermocouple near the sample but not in the path of the X-ray beam. A continuous record of the temperature was kept using a potentiometric recorder and the variation during an exposure was less than 3°K . The uncertainty in the temperature of the sample is, however, of the order of $\pm 10^{\circ}\text{K}$ because the thermocouple was not inside the capillary but was merely close to it.

The exposure times varied from one to twelve hours, due to differences in the intensities of the lines being observed and differences in the packing of the sample in the capillary. The capillary containing the sample was mounted on an axis perpendicular to the X-ray beam and was rotated about that axis while the photographs were being taken. The rotation of the capillary helped to ensure that reflections from all possible orientations of the crystals were recorded; as a result of this and the fineness of the powdered samples, the lines on the photograph showed no sign of spottiness but were uniform and easily measured.

2E. Spectroscopic Methods

The low-temperature infrared cell is illustrated in Figure 4 and consisted of two main parts: an inner part and an outer jacket. The inner part of the cell consisted of a copper block (D), which was machined to enable it to hold the infrared windows which contained the sample, a metal tank (B), and a copper tube (C) which connected the copper block to the tank. The tank was, in fact, a reservoir for liquid nitrogen which acted as a constant temperature coolant for the sample. The space between the inner part and the outer jacket was evacuated through the vacuum tap (A) and the vacuum seal between the two parts of the cell was provided by two greased buna-N O-rings. The windows (E) in the outer part of the cell were also vacuum-sealed using buna-N O-rings. Typically, the cell could be evacuated to 10 microns or better in 5 to 10 minutes. The window material used was polyethylene or teflon, and all of the windows were conically tapered with a half angle of $3^{\circ} 26'$ in order to eliminate interference fringes.

The far infrared samples consisted of the finely ground solid mulled with liquid propane at about 100°K. In the case of acetic acid II, powder X-ray photographs were taken of a different aliquot of the same powdered solid as was used for the infrared spectra, in order to confirm its

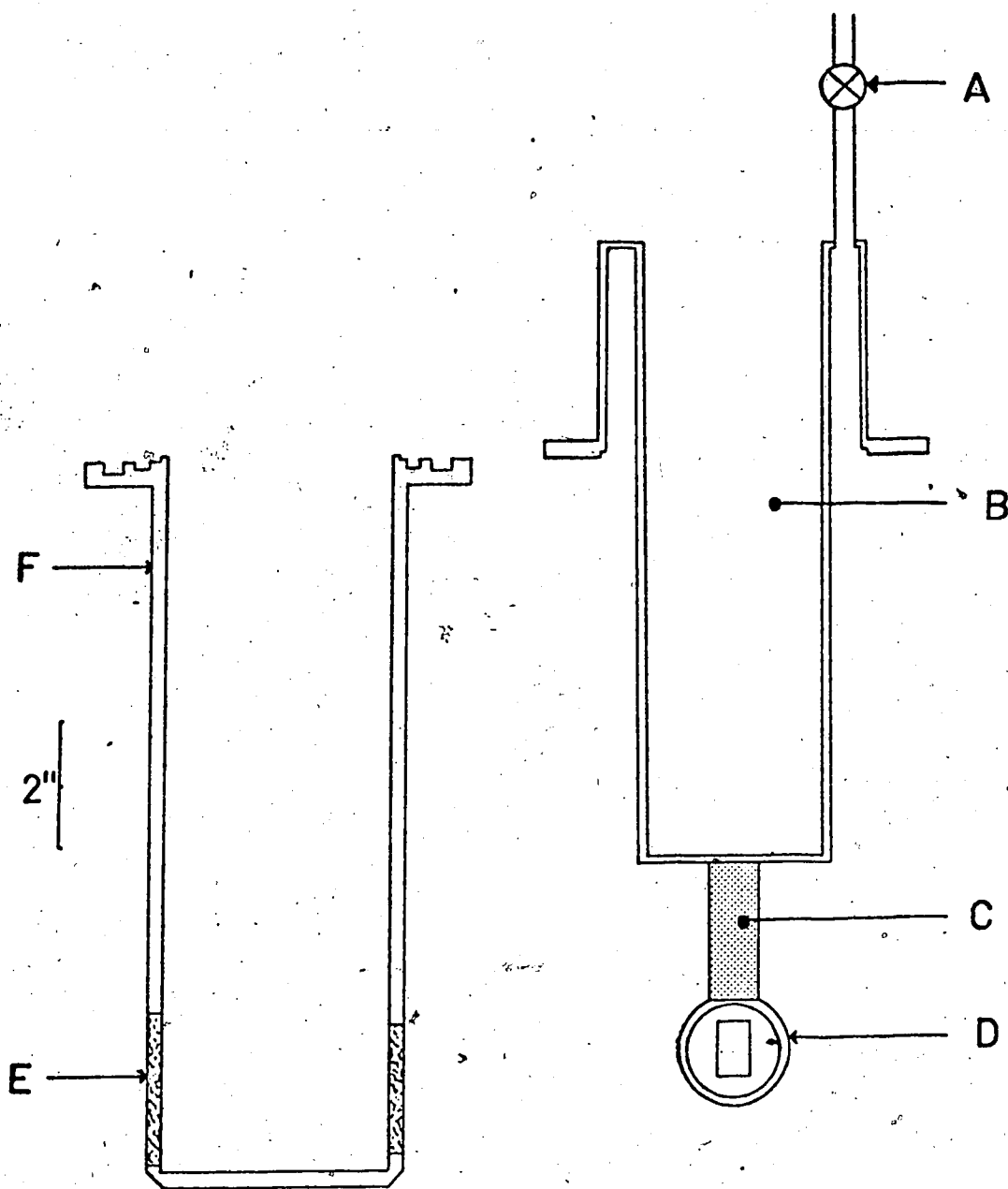


Figure 4. The cell used for low temperature infrared spectra. The lettered parts of the cell are as follows: A - the vacuum tap, B - the metal tank, C - the copper tube, D - the copper block, E - the outer-jacket windows and F - the solid metal wall of the outer jacket.

polymorphic state. The preparation of the powdered solids is described in Section 2C. The technique used to prepare low-temperature mulls was a modification of the technique developed by Bertie and Whalley(84) and is described below.

The mulls were prepared in a cold can which was specifically made for this purpose and was simply an uninsulated metal container with a metal platform in it. Below the level of the platform was a continuously boiling reservoir of liquid nitrogen. The walls of the cold can reached about 25 cm above the level of the platform, so that anything sitting on the platform was surrounded by an atmosphere of cold dry nitrogen gas. The inner part of the cell containing the windows, the vial for the mulling agent, and the stand for the windows, were cooled for one half hour in the cold can before the mulling process was begun. Since the liquid nitrogen was continuously boiling, more liquid had to be added to the reservoir from time to time, and the continuous flow of nitrogen gas out of the cold can prevented any condensation of water onto the cold apparatus within the can.

After the equipment in the cold can had been cooled, the windows were removed from the cell and laid flat on the window holder. The sample was then brought to the cold can from its storage dewar, and the vials were opened using long metal tweezers which had been cooled in liquid nitrogen. Then a long metal spatula, whose end had also been cooled in liquid nitrogen, was used to transfer some sample onto

one of the windows. The powdered sample was usually soaked in liquid nitrogen and had the texture of mud. However, once the sample was deposited onto the window, the nitrogen quickly evaporated leaving a little pile of the sample ready for mulling. The amount of sample needed for a mull varied greatly with the intensity of absorption required but was about 10 to 100 mg.

The mulling agent used was propane, which was condensed from a cylinder into a vial in the cold can. About 10 drops, or 0.5 cm^3 , of propane was usually condensed into the vial, and was then transferred to the sample on the window by dipping a long cold spatula into the liquid and touching the window with it. One or two drops of the mulling agent were thus placed on the window beside the sample, and within a few seconds spread over the window surface and into the sample. The spatula was then used to mix the powdered sample and the mulling agent together. The propane remained a liquid while in the cold can, even though the melting point of propane is 6° warmer than the boiling point of nitrogen.

It was found that the amount of propane used was crucial to obtaining a mull of the desired absorbance. Too little propane made the mull lumpy whereas too much propane washed the sample off the window when the windows were pressed together in the cell. When the correct amount of mulling agent was mixed with the powdered sample, it took

on the consistency of a thick slush and would flow somewhat on the windows but was not fluid enough to drain off.

In order, then, to obtain a smooth, uniform layer of sample on the window surface, the spatula was used to spread out the material into approximately the desired position. Then the other window was set on top of the mull to sandwich it between the two windows. The top window had a small indent into which the points of a cold pair of tweezers were placed, and the top window was rubbed over the bottom one to do the final smoothing of the mull. If this process was continued too long, though, it tended to squeeze the mull out from between the windows. Since polyethylene or teflon windows were used it was not possible to see the actual mull, and this made it difficult to know when to stop smoothing but with experience, this method gave very good mulls which consistently had the desired absorbance.

⑦ Once the mull was prepared, the windows were mounted into the copper block and held in place by squeezing them between two copper surfaces, in the center of which were rectangular apertures. The one surface was part of the copper block whereas the other surface was removeable and was held in place by a spring soldered to a copper ring which, in turn, was screwed to the copper block. At this point the inner part of the cell and the outer jacket were ready to be joined. The outer jacket, which was warm and

which had been purged for at least one half-hour with dry nitrogen gas, was placed into a special side arm of the cold can which was also filled with dry, cold nitrogen gas. To make sure that the sample remained cold, a small amount of liquid nitrogen was poured into the tank of the inner part of the cell. The two parts were then joined ensuring that the copper block containing the sample stayed inside the cold, dry atmosphere; the vacuum tap was opened and the cell was removed from the cold can. The liquid nitrogen tank was then completely filled and the cell was allowed to stand until it was evacuated to a pressure of 10 microns. Since the windows in the cell were opaque to visible light, the windows containing the sample were aligned parallel to the outer windows by rotating the inner part until marks on the two parts of the cell were aligned.

When the pressure in the cell was 10 microns, the vacuum tap was closed and the cell was taken to the interferometer where it was connected to another vacuum line to ensure that the pressure stayed below 10 microns. The liquid nitrogen tank of the cell required refilling every three hours but normally it was kept at least half full all of the time.

Far infrared interferograms were obtained from a Beckman-RIIC FS720 interferometer, equipped with a continuous, Moire drive system (85). Five mylar beam splitters of thickness 6, 12, 24, 48 and 96 microns, were

used in conjunction with four high-frequency cut-off filters in order to investigate the spectral region from 360 to 10 cm^{-1} . The interferometer was evacuated to at least 50 microns to remove water vapor before interferograms were recorded, but the pressure was usually less than 20 microns. The pressure in the interferometer, and that in the cell, were continuously monitored using model G6A Pirani Gauge Heads connected to model B5 Speedivac-Gauges.

The interferograms consisted of the intensity of radiation reaching the Golay Detector at uniformly spaced values, between $+X$ and $-X$ cm, of the path difference between the two beams of the interferometer (86, 87). The intensities were digitized and automatically punched onto computer cards. They were then Fourier-transformed by the I. B. M. model 360/67 computer, using the program BOBS IV which was written in this laboratory by Bertie, Othen, Brooks and Sunder. The program, written originally in Fortran IV, performs sine and cosine Fourier transformations of the intensities and determines the intensity at wave number ν as the square root of the sum of the squares of the sine and cosine transforms at that wave number. In simple terminology this procedure transforms the intensities from the distance domain (an interferogram) to the wave number domain (a spectrum) (88). In order to prevent spurious peaks from being introduced into the spectra so obtained because of the truncation of the interferograms,

the interferograms were apodized using a triangular apodizing function (86).

The BOBS IV program allows the interferograms to be transformed singly, and plotted as intensity versus wave number or sample and reference interferograms may be used and the resulting spectra are ratioed to yield a plot of absorbance versus wave number. Further, the program allows several absorbance spectra to be averaged together to reduce noise, and the averaged spectrum is plotted. When a reference interferogram was desired the cell was prepared in the way described earlier, except that only propane was placed between the windows.

The resolution obtained in the spectra equals $1/X$ cm^{-1} , where X cm is the maximum path difference, if the interferogram is not apodized. However, triangular apodization lowers the resolution by 50% so the resolution in this work was given by $1.5/X$ cm^{-1} . The resolution used in the region 350 to 100 cm^{-1} , which was covered in a single interferogram taken with the 6 micron thick beam splitter, was 3.0 cm^{-1} . But below 100 cm^{-1} , where the 12, 24, 48 and 96 micron beam splitters were used, the resolution was better than 2.0 cm^{-1} . This is because the path difference between sampling points must be less than or equal to $1/2 \nu_{\text{max}}$, so that when only low frequencies are studied the sampling interval is increased making it convenient to increase the maximum path difference (and resolution) without increasing

the number of data points. The frequency accuracy of the interferometer has been calibrated several times by others in this laboratory (89). The spectra of water vapor, hydrogen chloride and methanol oxide have shown the frequency to be accurate to at least $\pm 0.2 \text{ cm}^{-1}$.

The temperature of the sample was not measured but it can be estimated in the following way. The melting point of propane is 83°K (5) and the vapor pressure of propane is about 10 microns at 103°K and 0.01 microns at 77°K (84). Therefore, if the temperature of the samples had been higher than 100°K , the propane would have evaporated, and below 83°K it would have solidified.

When the cell was dismantled after taking spectra, propane was always found in the mull, and if the propane had solidified while a spectrum was being recorded a significant drop in intensity would have been observed. The conclusion being, then, that the temperature of the mulls was in the range $92 \pm 10^\circ\text{K}$.

Chapter 3. The Phase Diagram of Acetic Acid Below 0°C

The methods used to study the phase diagram of acetic acid below 0°C and the results obtained are presented and discussed in this chapter.

3A. Methods

The acetic acid was put into the high-pressure cell and pressurized in the way described in Section 2B. After the apparatus had stabilized at the desired temperature, the pressure was increased by 50 to 100 bars every eleven minutes, and the dial gauge and pressure readings were taken ten minutes after the pressure change (measured by stop-watch). This time period was chosen because the slow changes in the pressure and dial gauge readings which always follow a pressure change had become extremely slow after 10 minutes. The onset of the acetic acid I to II phase transition was indicated by a deviation of the dial gauge readings from the line formed by the data previously taken on a graph of pressure against dial gauge readings. Once the phase transition began to occur, dial-gauge and pressure readings were taken every 10 minutes without pumping any oil into the press until the phase transition was completed or until the pressure became steady. The pressure was then increased in the usual way a few hundred bars past the phase transition and then allowed

to sit for at least one hour before the pressure was decreased. The entire phase transition took between 30 and 50 minutes and the platten movement amounted to about three thousandths of an inch. The acetic acid II to I phase transition was then measured in the same way, except that oil was removed from the press by way of a release valve rather than pumped into the press.

When the phase transition measurements were completed, the pressure was released until the upper piston no longer touched the top platten. At that point the zero pressure reading was read from the pressure gauge. The usual zero pressure reading was 1.2 to 1.4 bars oil pressure and was subtracted from all pressure readings taken during the measurements.

One of the limitations in the quality of the results obtained was the difficulty in recognizing that the transition had started in time to study it in detail. A phase transition often does not start until the pressure is somewhat higher than that required to keep the transition occurring once it has started, but once the transition is initiated, the pressure drops back and the pistons move closer together. Accurate measurements of the transition pressure can be obtained if the pressure is allowed to drop as far as it will, then the pressure

is increased slightly by pumping more oil into the press and the pressure is allowed to drop as far as it will, and this process is repeated with the pressure dropping to the same value each time. For the acetic acid I to II transition studied in this work, however, the volume change at the transition was only about 1.5% of the volume at atmospheric pressure, so the transition was often very nearly completed by the time the pressure had dropped from that which was required to initiate the transition. When the pressure was then raised slightly, the transition was completed and the pressure did not drop back to the same pressure as it reached on its initial drop. This is illustrated by the graph of pressure against volume change shown in Figure 5. In this case one can only select the single point at the lowest pressure reached during the I to II transition and assume that it is the correct minimum pressure required to keep the I to II transition running. The same principles apply when the II to I transition is being measured, but the effect is the reverse of that experienced in the I to II transition, as shown in Figures 5 and 6. The transition pressure was somewhat better defined during other measurements in this work, an example of which is shown in Figure 7, but an un-

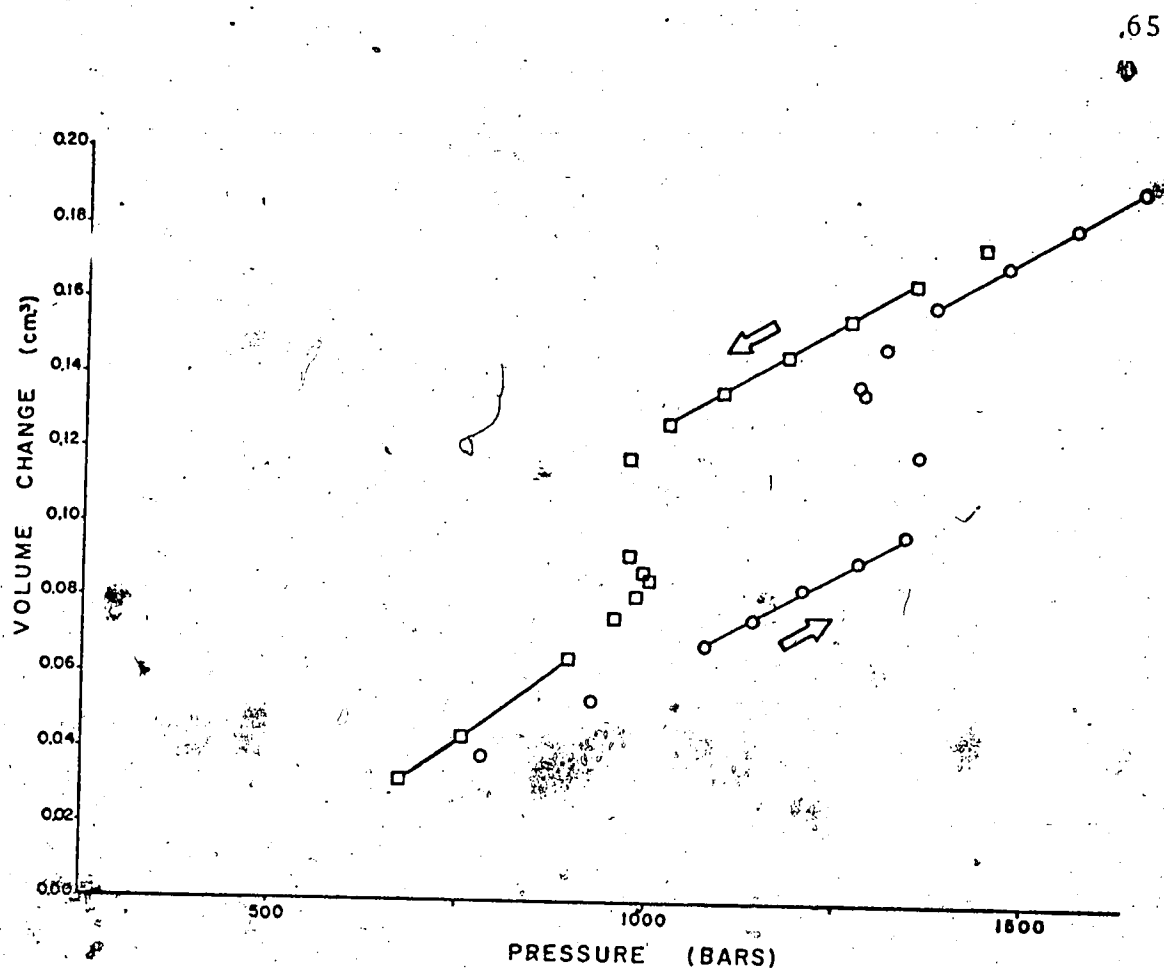


Figure 5. Graph of volume change vs. pressure for the phase transition occurring at 0°C. The arrows indicate the sequence in which consecutive points were taken. The points represented by circles illustrate the increasing pressure phase transition and the squares represent the decreasing pressure phase transition.

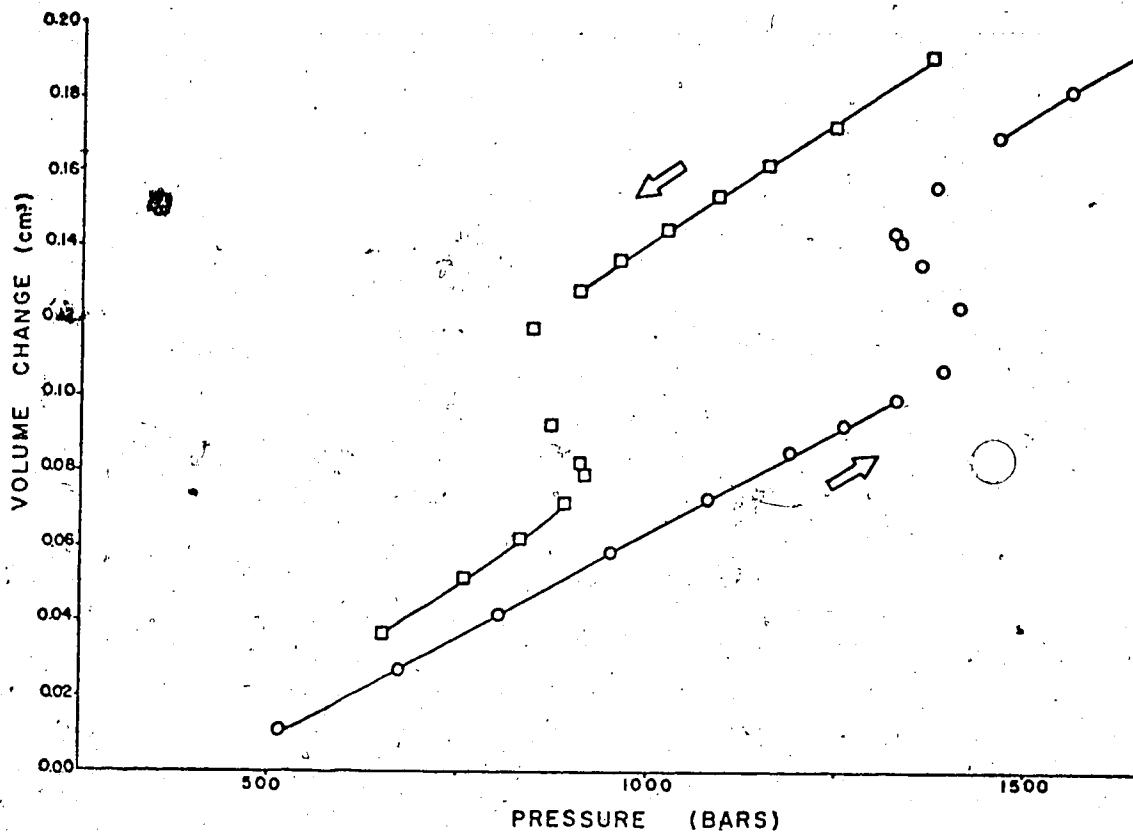


Figure 6. Graph of volume change vs. pressure for the phase transition occurring at 0°C. The arrows indicate the sequence in which consecutive points were taken. The points represented by circles illustrate the increasing pressure phase transition and the squares represent the decreasing pressure phase transition.

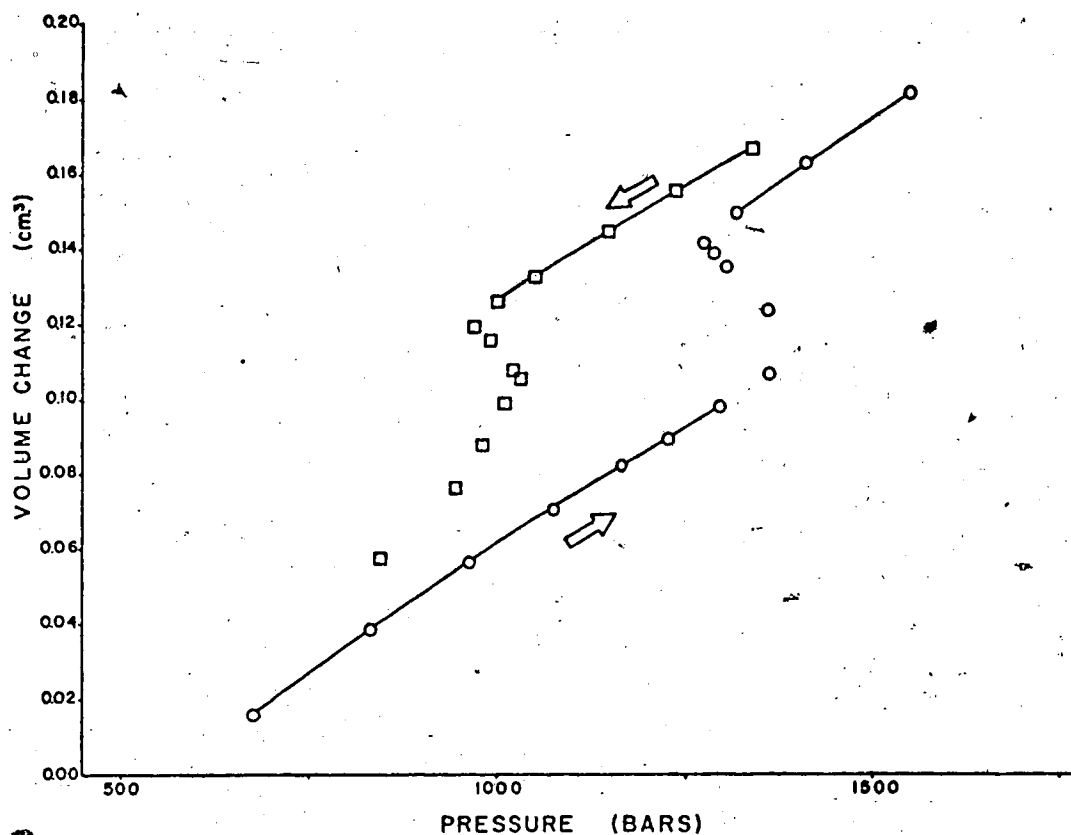


Figure 7. Graph of volume change vs. pressure for the phase transition occurring at 0°C. The arrows indicate the sequence in which consecutive points were taken. The points represented by circles illustrate the increasing pressure phase transition and the squares represent the decreasing pressure phase transition.

certainty does remain in the results because of this effect. In order to minimize the effect, the piston in the hydraulic ram was kept very close to the bottom of the ram, to minimize the volume of compressed oil under the piston. The use of relatively long samples to maximize the linear displacement during the transition also relieves this problem. The samples used were between three and four millimeters long. This length was chosen because with shorter samples the piston movement was too small to be precisely measured and with longer samples the frictional effects due to non-hydrostatic conditions became so large that no advantage was gained.

3B. Results and Discussion of the Phase Diagram Work

The transition pressures of the acetic acid I to II and II to I phase transitions were obtained at several temperatures by the methods described in Sections 2B and 3A, and are presented in Table 7 and Figure 8. The equilibrium pressure is usually (90) found by averaging the pressures of the I to II and the II to I transitions, on the assumption that the hysteresis effects are symmetrical. The equilibrium pressures so obtained are also listed in Table 7 and shown in Figure

Table 7. Phase Diagram of Solid Acetic Acid

Temperature (°C)	Lower Transition (bars)	Upper Transition (bars)	Equilibrium Transition Pressure \pm Standard Deviation (bars)	No. of runs
15.5 ^a	1168	1629	1399	1
11.6	1164	1493	1329	1
3.8	1007	1370	1189	1
0.0 \pm 0.3	977	1293	1135 \pm 18	10
-10.0 \pm 0.3	677	1186	931 \pm 28	7
-20.0 \pm 0.3	412	1066	739 \pm 39	3
-26	268	1307	788	1
-31	84	1591	838	1
-34	40	(2300-2700) ^b	838	1

^a These transitions were measured by taking readings every 5 minutes instead of the 11 minutes used for the other transitions.

^b The transition was extremely sluggish and not well defined.

(Table continued)

Table 7 continued

Other Workers:

	<u>Temperature (°C)</u>	<u>Equilibrium Transition Pressure (bars)</u>
Tamman	10.01	130.7±69
	0.00	1123±25°
	-20.7	750±83
Bridgman	0.0	1064

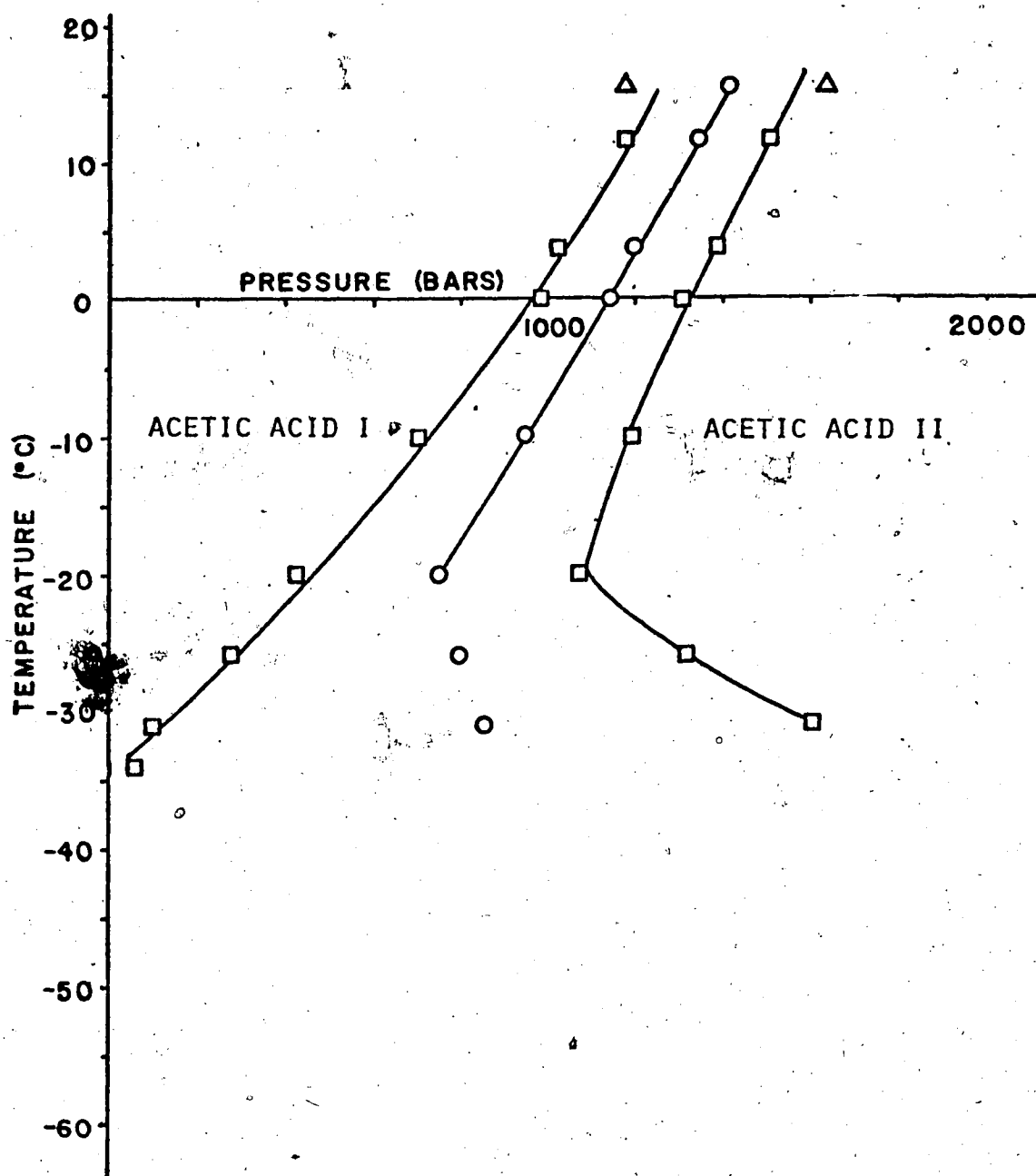


Figure 8. The pressure-temperature phase diagram of solid acetic acid. The circles represent the equilibrium phase transition line and the squares and triangles represent the observed phase transitions. If the time interval between readings was 11 minutes, a square is used, if 6 minutes a triangle is used.

8, and where indicated, the pressures listed are the average of the values obtained at that temperature.

The transition pressures were read from graphs of the volume change plotted against pressure with a precision of ± 2 bars, but the reproducibility found in different experiments at the same temperature decreased as the temperature was lowered but was of the order of ± 25 bars. Better reproducibility might have been achieved if the piston had been oscillated to reduce friction.

The equilibrium transition pressure found at 0°C is useful for comparison with those of previous workers. Tammann (2) reported 1145 Kg/cm^2 , which is equivalent to 1123 bars, and Bridgman (3) reported 1074 Kg/cm^2 which, when corrected for the error in his pressure calibration (91,92), is 1085 Kg/cm^2 and is equivalent to 1064 bars. The value 1135 bars reported in his work is the average of ten experiments, and has been carefully checked because it is higher than either of those previously reported. Bridgman claimed that his samples were more pure than those of Tammann (2) and assumed that the greater purity resulted in a lower and more correct phase transition pressure. In order to check Bridgman's (3) claim, three experiments were done using a sample to which a small amount of water had been

added. The result was that the pure samples gave an equilibrium transition pressure 20 bars higher than the impure samples. This experimental evidence, along with the fact that this work agrees reasonably well with that of Tammann (2) (Table 7) and that the pressures at other temperatures with different samples are consistent with a transition pressure of 1135 bars at 0°C , provides the basis for concluding that Bridgman's (3) value for the transition pressure at 0°C is incorrect. This is not entirely surprising since Bridgman (3) only did a single experiment to measure the phase transition at 0°C .

It is clear from the results presented in Figure 8 that acetic acid II can not be formed from acetic acid I at less than about 800 bar in a reasonable time. The reason for the sharp increase in the I to II transition pressure as temperature decreases is not known, but it could well be due to a rapid decrease in the rate of the transition with decreasing temperature, and is probably not an equilibrium effect. Acetic acid II is metastable up to about -35°C at atmospheric pressure and judging from the extrapolation of the equilibrium line, phase II is the stable phase below about -60°C at one atmosphere, even though it can not be formed by

cooling phase I to that temperature.

The thermodynamic parameters for the transition were also calculated and compared with those reported by Bridgman (3) as shown in Table 8. The slope of the equilibrium line of the phase transition, dP/dT , equals 18.2 ± 0.9 bars/degree whereas the value reported by Bridgman (3) was 18.4 bars/degree. Using the Clapeyron equation: $\Delta S = \Delta V \cdot dP/dT$, it is possible to calculate ΔS , the entropy of acetic acid II minus that of acetic acid I, and hence to calculate ΔH , the enthalpy change, since the free energy is constant during a reversible phase transition and $\Delta H = T\Delta S$. The values measured for ΔV , the volume of phase II minus that of phase I, were taken from graphs similar to those shown in Figures 5, 6, and 7, with an uncertainty of about $\pm 0.003 \text{ cm}^3$ which, corrected for the mass of the sample, corresponds to $\pm 0.0007 \text{ cm}^3/\text{g}$. Bridgman's (3) value of $0.0140 \text{ cm}^3/\text{g}$, for the volume change at 0°C agrees with the value obtained in this work, $0.0138 \text{ cm}^3/\text{g}$, within the specified uncertainty. Table 8 gives the thermodynamic parameters of the phase transition calculated at 0, -10 and -20°C , and the uncertainty in the values listed is about 7 or 8%.

Table 8. Thermodynamic Parameters for the Solid Acetic Acid Phase Transition

Temperature (°C)	ΔV (cm ³ /g)	ΔS (cal/mole deg.)	ΔH (cal/mole)
0	-0.0138	-0.361	-98.5
-10	-0.0141	-0.368	-97.0
-20	-0.0143	-0.374	-94.6

Bridgman's reported values: $dp/dT_s = 18.4$ bars/degree

0	-0.0140	-0.369	100.8
---	---------	--------	-------

Chapter 4. A Discussion of the X-ray Measurements on

Acetic Acid Powdered Solids

The X-ray diffraction patterns of powdered acetic acid I and acetic acid II are discussed in this chapter to interpret and evaluate the data obtained.

Samples of acetic acid I and II were prepared, and X-ray diffraction patterns were obtained as described in Sections 2C and 2D. Four diffraction pattern photographs were taken of acetic acid I, using $\text{CuK}\alpha$ radiation, in order to evaluate the results obtained using powder techniques by comparing them with those obtained from single crystals, and in order to distinguish between the diffraction patterns of acetic acid I and acetic acid II. Eight photographs of the acetic acid II diffraction pattern were obtained, five using $\text{CuK}\alpha$, two using $\text{CoK}\alpha$ and one using $\text{CrK}\alpha$ radiation.

These photographed X-ray diffraction patterns consisted of concentric rings whose inside and outside diameters were measured and averaged to obtain the diameter of the ring, D . The diffraction angle, θ , was calculated from the equation

$$D/2S = \tan 2\theta$$

where S is the sample-to-film distance, 60.0 mm. The

inter-planar spacings, usually called the d-spacings, d , were then calculated from the Bragg Equation

$$d = \lambda / 2 \sin \theta$$

where λ is the wavelength of the diffracted radiation. The values obtained for the d-spacings of acetic acid I and II are listed in Tables 9 and 10, respectively. The patterns were clearly distinct and allow acetic acid II to be recognized.

The relative intensities of the lines produced by radiation diffracted by acetic acid II were measured by a Joyce MK. III C double beam recording microdensitometer. The areas under the peaks on the microdensitometer trace were taken to be proportional to the line intensities, and the intensities in Table 10 were obtained by multiplying the ratio of the area under a peak to the area under the largest peak by 100.

The observed d-spacings for acetic acid I at 100°K were indexed using the Hesse-Lipson method (93, 94) in which the diffraction lines of a powdered unknown orthorhombic crystal can be assigned Miller indices, h , k , and l . The indexed lines were used to calculate the unit cell parameters which were refined by a least squares procedure using the computer program DREFINE

Table 9. X-ray Powder Diffraction Data for Acetic Acid I at 100°K and Atmospheric Pressure.

line	d(Å) observed ± mean deviation	d(Å) calculated	d _{obs} - d _{calc.} (Å)	hkl	no. of photographs
1	6.641±0.018	6.626	0.015	200	4 Cu
2	4.348±0.011	4.359	-0.011	201	4 Cu
3	3.391±0.004	3.374	0.017	210	4 Cu
4	3.257±0.003	3.246	0.011	011	4 Cu
5	3.155±0.004	3.152	0.003	111	4 Cu
6	2.917±0.013	2.915	0.002	211	3 Cu
7	2.857±0.005	2.875	-0.018	401	2 Cu
8	2.628±0.004	2.611	0.013	311	3 Cu
9	2.300±0.005	2.292	0.008	112	4 Cu
10	2.174±0.003	2.179	-0.005	402	4 Cu
11	2.055±0.001	2.053	0.002	511	4 Cu
12	1.955±	1.960	-0.005	020	1 Cu
13	1.928±	1.939	-0.011	120	1 Cu
14	1.902±0.001	1.905	-0.003	412	2 Cu
15	1.844±0.001	1.839	0.005	121	2 Cu
16	1.798±	1.792	0.006	320	1 Cu

(Table continued)

Table 9 continued

Acetic Acid I unit cell parameters
orthorhombic; 4 molecules/unit cell

278°K*	100°K	83°K*
$a = 13.310 \pm 0.001 \text{ \AA}$	$a = 13.25 \pm 0.05 \text{ \AA}$	$a = 13.214 \pm 0.001 \text{ \AA}$
$b = 3.90 \pm 0.001 \text{ \AA}$	$b = 3.92 \pm 0.01 \text{ \AA}$	$b = 3.924 \pm 0.001 \text{ \AA}$
$c = 5.769 \pm 0.001 \text{ \AA}$	$c = 5.79 \pm 0.02 \text{ \AA}$	$c = 5.766 \pm 0.001 \text{ \AA}$
$V = 78.5 (\text{\AA})^3$	$V = 75.2 (\text{\AA})^3$	$V = 74.8 (\text{\AA})^3$

V = molecular volume

* Data taken from reference 18

Table 10. X-ray powder diffraction data for acetic acid II at 100°K and atmospheric pressure

line	Relative Intensity	d(Å) observed ± mean deviation	d(Å) calculated	d _{obs} - d _{calc.} (Å)	hkℓ	no. of photographs
1	44.7	6.610±0.018	6.632	-0.022	200	5Cu, 2Co, 1Cr
2	39.4	5.208±0.007	6.614	-0.004	011 (a)	
3	32.7	4.304±0.011	5.198	0.010	020	5Cu, 2Co, 1Cr
4	39.2	3.480±0.007	4.287	0.017	002	5Cu, 2Co, 1Cr
			3.493	-0.013	202 (a)	5Cu, 2Co, 1Cr
			3.465	0.015	030	
5	62.1	3.353±0.006	3.353	0.000	130	5Cu, 2Co, 1Cr
6	~ 0.1	3.222±0.009	3.213	0.009	031	1Cu, 2Co, 1Cr
7	11.0	3.128±0.006	3.141	-0.013	131	5Cu, 2Co, 1Cr
8	100.0	3.036±0.004	3.048	-0.012	312	5Cu, 2Co, 1Cr
			3.029	0.007	411 (a)	
9	8.8	2.956±0.007	2.978	-0.022	302	5Cu, 2Co, 1Cr

(Table continued)

Table 10 continued

line	Relative Intensity	d(A) observed ± mean deviation	d(A) calculated	d _{obs} - d _{calc.} (Å)	hkl	no. of photographs
10	8.3	2.842±0.005	2.834	0.008	103	5Cu, 2Co
11	8.3	2.766±0.005	2.755	0.011	013	5Cu, 2Co
12	7.0	2.655±0.002	2.755	0.011	103(a)	
			2.653	0.002	500(a)	5Cu, 2Co
			2.663	-0.008	113	
			2.663	-0.008	132	
13	7.5	2.600±0.002	2.599	0.001	040(a)	5Cu, 2Co
			2.606	-0.006	213	
14	26.8	2.380±0.001	2.390	-0.010	223	5Cu, 2Co
15	26.8	2.334±0.001	2.337	-0.003	431(a)	5Cu, 2Co
			2.329	0.005	303	
			2.303	0.006	502	

(Table continued)

Table 10 continued

line	Relative Intensity	d(A) observed \pm mean deviation	d(A) calculated	d _{obs} - d _{calc.} (A)	hkl	no. of photographs
16	8.4	2.265 \pm 0.003	2.259	0.006	332(a)	5Cu, 2Co
			2.272	-0.007	512	
			2.273	-0.008	313	
17	2.0	2.195 \pm 0.002	2.194	0.001	133(a)	5Cu
			2.191	0.004	413	
18	2.2	2.106 \pm 0.000	2.106	0.000	530	5Cu
19	2.2	2.064 \pm 0.001	2.064	0.004	233	5Cu
20	0.3	1.982 \pm 0.002	1.982	0.000	304(a)	3Cu
			1.981	0.001	024	
			1.984	-0.002	250	
21	6.2	1.924 \pm 0.002	1.924	0.000	251(a)	5Cu
			1.923	0.001	043	
22	0.7	1.866 \pm 0.001	1.867	-0.001	224	5Cu

(Table continued)

Table 10 continued

line	Relative Intensity	d(A) observed \pm mean deviation	d(A) calculated	d _{obs.} - d _{calc.} (A)	hkl	no. of photographs
23	1.3	1.835 \pm 0.001	1.833	0.002	541	5Cu
24	2.9	1.786 \pm 0.001	1.787	-0.001	252(a)	5Cu
25	1.2	1.760 \pm	1.784	0.002	234	
			1.761	0.001	450	1Cu

(a) indicates the indices used in the DREFINE program where more than one assignment is given

Unit cell parameters of acetic acid II

16 molecules/unit cell

$$a = 13.30 \pm 0.02 \text{ \AA}$$

$$b = 10.39 \pm 0.01 \text{ \AA}$$

$$c = 8.59 \pm 0.01 \text{ \AA}$$

$$\text{molecular volume} = 74.1 \text{ \AA}^3$$

$$\alpha = 90.0^\circ$$

$$\beta = 86.1 \pm 0.3^\circ$$

$$\gamma = 90.0^\circ$$

(95): The refined unit cell parameters were then used to calculate d-spacings and the differences between the observed and calculated d-spacings (column 4 of Table 9) were used as an indication of the reliability of the derived cell parameters, which are compared in Table 9 with parameters obtained from single crystal work at 278 and 83°K (18). The agreement is good. The uncertainties in the cell parameters at 100°K were calculated by the program DREFINE.

The diffraction patterns expected for acetic acid I at 278°K and 83°K were calculated from data reported by Nahrngbauer (18), as shown in Table 11, and were compared with that found in this work to determine the reliability of the powder method. The line intensities were calculated as the integrated cross-sectional optical density by the equation (96)

$$I_{hkl} \propto m F_{hkl}^2 \left[\frac{1 + \cos^2 2\theta}{\sin^2 \theta \cos \theta} \right] \cos 2\theta$$

where m is the multiplicity and F_{hkl} is the structure factor of the reflection plane. The line intensities observed agree qualitatively with those calculated, and it is clear that many lines on the powder pattern are due to more than one set of reflections.

Table 11. Powder diffraction patterns of Acetic Acid I
at 278 and 83°K, calculated from the cell
parameters and structure factors reported by
Nahringbauer (18)

line	hkl	278°K		83°K	
		d(Å)	Relative Intensity	d(Å)	Relative Intensity
1	200	6.660	89	6.607	72
2	201	4.361	100	4.348	100
3	210	3.479	25	3.377	53
4	011	3.331	35	3.247	47
	400	3.327	13	3.303	10
			48		57
5	111	2.231	44	3.155	52
6	310	2.007	4	2.933	4
	211	2.983	32	2.917	28
			36		32
7	401	2.886	14	2.869	11
	002	2.885	4	2.883	2
			18		13
	311	2.669	27	2.617	37
	202	2.649	29	2.644	31
			56		68
9	112	2.322	10	2.291	8
	411			2.318	2
					10
10	402	2.182	15	2.174	17
11	312	2.082	4	2.059	3
			14		13
	511	2.081	10	2.052	10

(Table continued)

Table 11 continued

line	hk ℓ	278°K		83°K	
		d(Å)	Relative Intensity	d(Å)	Relative Intensity
12(a)	020				
13	120	2.016	2	1.941	3
14	412	1.924	3	1.904	4
15	121	1.904	5	1.841	6
16	320	1.854	2	1.793	3
	221	1.851	1		
	203	1.848	2		

(a) structure factors were not given for this reflection.

Even though the unit cell symmetry of acetic acid II was unknown, the Hesse-Lipson method was applied in an attempt to index the diffraction pattern on the basis of orthorhombic symmetry. The lines were indexed and cell parameters were calculated, but the agreement between calculated and observed d-spacings was significantly poorer than that found for acetic acid I. Further, the calculated molecular volume was approximately 5% larger than that found for acetic acid I under the same conditions, instead of being about 1.5% smaller as was expected since the volume change at the phase transition at 0°C was found to be about 1.5% (Chapter 3 and reference 3). However, it was subsequently found that by allowing the unit cell to have monoclinic symmetry and reassigning some of the diffraction pattern lines, much better agreement between observed and calculated d-spacings was obtained and the molecular volume was approximately 1.5% smaller than that of acetic acid I under the same conditions. Therefore, it was concluded that the unit cell given in Table 10, containing 16 molecules and having monoclinic symmetry, provides an adequate fit and is the best fit obtainable using these methods.

Chapter 5. The Far Infrared Spectra of Acetic I, Acetic Acid II and Propionic Acid

The far-infrared spectra obtained in the present work are presented in Section 5B and discussed in Section 5C. Section 5A presents a theoretical analysis of the inter-monomer vibrations of acetic acid I, which has not been presented previously and is required in order to attempt to assign the spectrum in a more satisfactory way than has been done previously.

5A. Analysis of the inter-monomer vibrations of acetic acid I

As was described in Section 1D, acetic acid I is known to exist as long chain hydrogen-bonded polymers, which crystallize in the space group $Pna2_1-C_{2v}^9$, with two monomers in each of two chains in the unit cell. The unit cell group (64) is isomorphous to the point group C_{2v} .

The absorption by the internal vibrations of the acetic acid monomer units can be analyzed by considering only a single chain, as discussed in Section 1D. The implication of this is that the hydrogen bond forces within a chain are much more important than the van der Waals' forces between the chains. If only a

single chain is considered, there are two monomers per unit cell and the unit cell group is isomorphous with the point group C_s , in which all the vibrations are infrared active. If the single-chain approximation is applied to the inter-monomer vibrations, twelve vibrations are expected, but three of them are the simple translations of the chain and another is a simple rotation of the chain and the frequencies of these four vibrations must be assumed to be very small compared to those of the other eight vibrations. These eight remaining vibrations of a single chain involve bending and stretching of the hydrogen bond and are expected to have frequencies above about 50 cm^{-1} . In polyethylene the inter-chain vibrations have frequencies between 70 and 100 cm^{-1} , so it must be anticipated that the inter-chain vibrations of acetic acid will have similar frequencies. Therefore the single-chain approximation is not expected to be useful for the inter-monomer vibrations and the full unit cell must be taken into account.

In acetic acid I, the twelve inter-monomer vibrations of the single chain become twenty-four vibrations in the full unit cell, three of which are the simple translations of the unit cell and have zero frequency.

The remaining twenty one vibrations form the representation $5A_1 + 6A_2 + 5B_1 + 5B_2$ but since the A_2 modes are infrared inactive only fifteen vibrations are expected to absorb in the far infrared region.

The single chain approximation is, however, useful to help one to visualize the zero-wave-vector lattice vibrations of the crystal and to estimate their frequencies. Figure 9 shows the twelve zero-wave-vector symmetry coordinates of a single chain which are based on translational and rotational motions of the molecule. The dotted lines enclose the molecules within one unit cell and the dot-dashed line shows the diagonal glide plane which, apart from the identity, is the sole symmetry element of the chain. This glide plane lies in the crystal's bc plane, and the dot-dashed line in Figure 9 lies along the crystal's $\underline{b} + \underline{c}$ direction. The translational displacements are, for brevity, termed x , y and z displacements and correspond to displacements in the crystal's $\underline{b} + \underline{c}$, \underline{a} and $\underline{b} - \underline{c}$ directions. The rotational displacements are about the inertial axes of the monomer and are termed rotations about m , n and z . The symmetry coordinates for the full unit cell are derived from those of a single chain simply by considering the 2_1 screw axis symmetry operation. If the

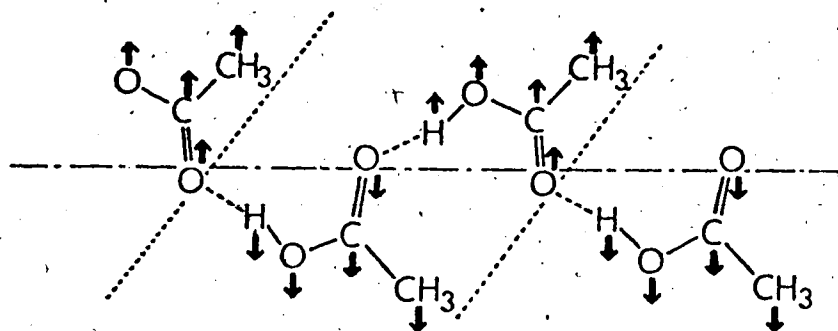
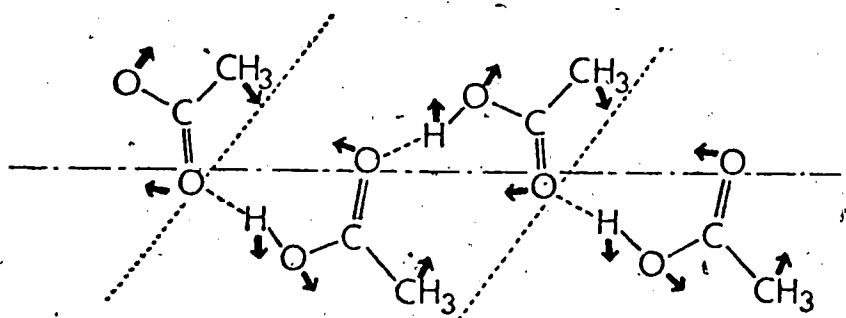
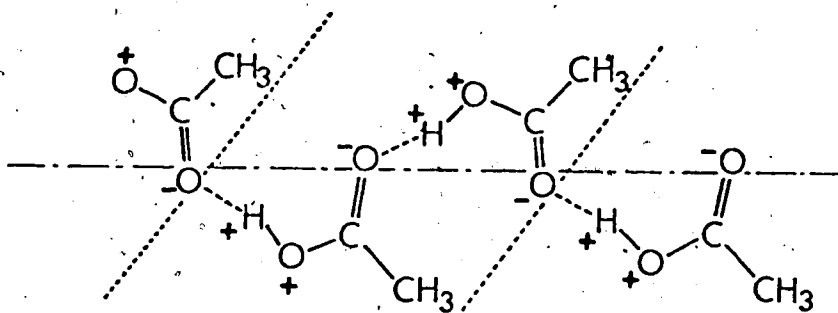
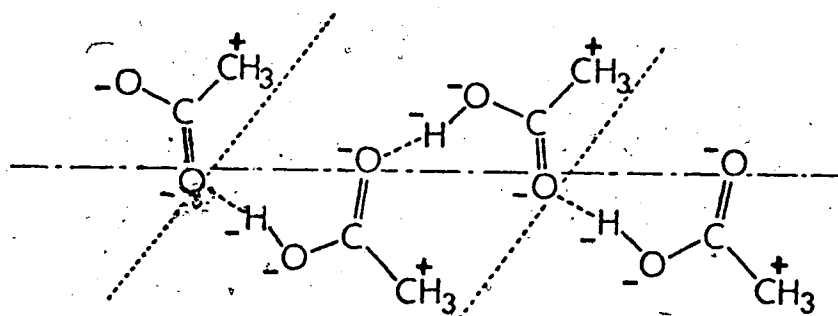

 T_y
 $S_1(A')$

 R_z
 $S_2(A')$

 R_m
 $S_3(A')$

 R_n
 $S_4(A')$

Figure 9. Symmetry coordinates for a single chain in acetic acid I. The arrows indicate motion in the plane of paper and the plus and minus signs indicate motion out of the plane.

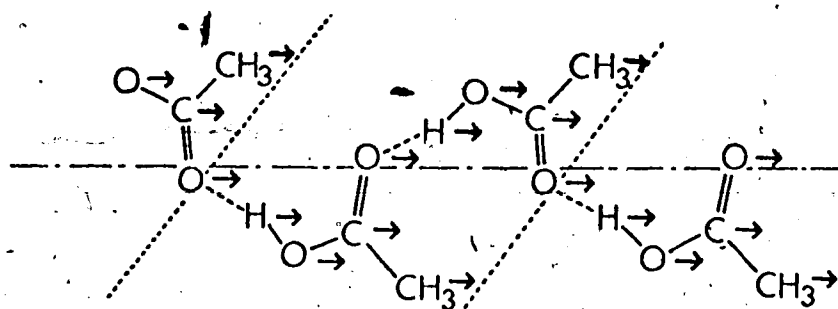
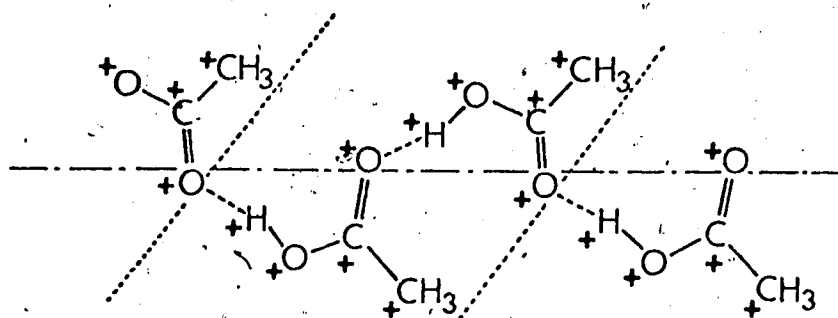
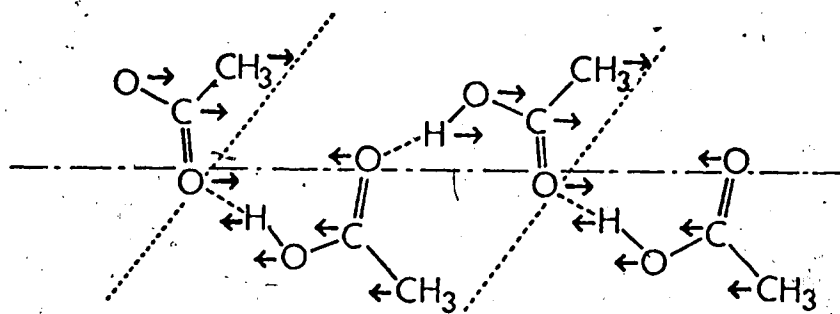
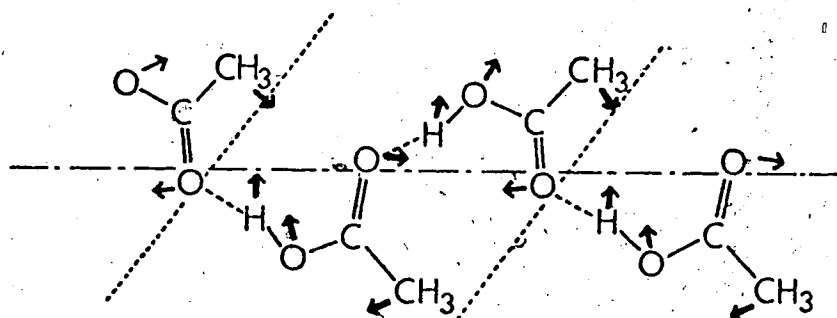

 T_x
 $S_5(A')$

 T_z
 $S_6(A')$

 $T_{x'}$
 $S_7(A'')$

 $R_{z'}$
 $S_8(A'')$

Figure 9 continued

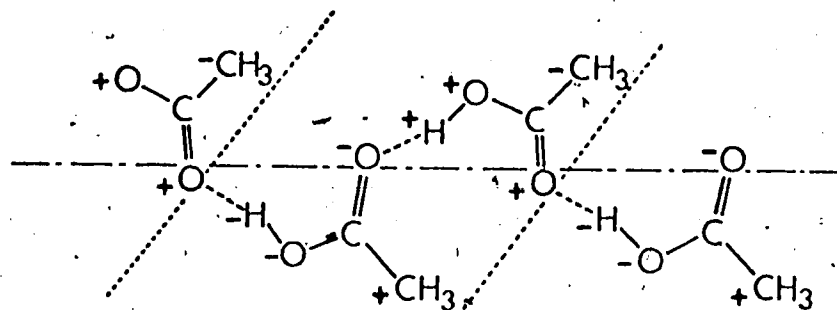
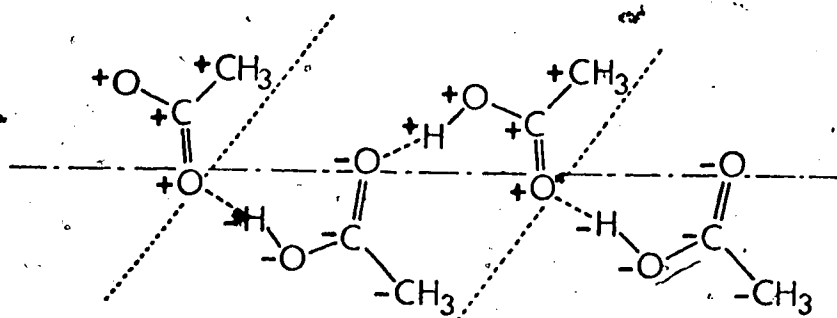
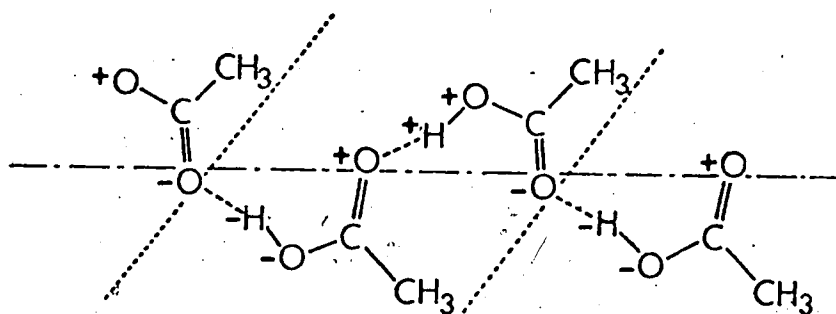
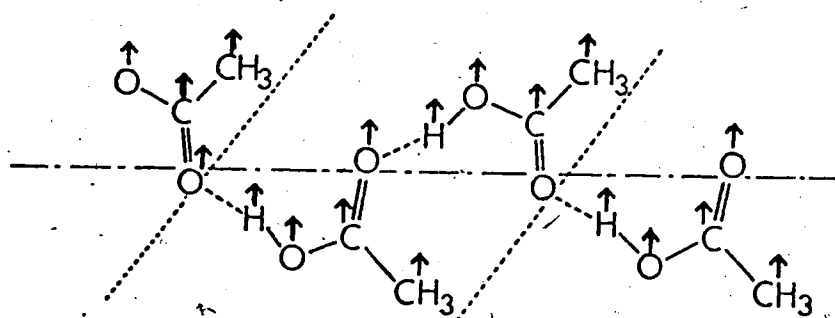

 R'_n
 $S_9(A'')$

 T'_z
 $S_{10}(A'')$

 R'_m
 $S_{11}(A'')$

 $T'_{y'}$
 $S_{12}(A'')$

Figure 9 continued

displacements having A' symmetry in each chain may be reproduced in the other by application of the screw axis operator, then the symmetry coordinate produced has A_1 symmetry in the full unit cell. If the displacements so produced have opposite sign, then the symmetry coordinate produced has B_1 symmetry. Similarly displacements having A'' symmetry in each chain produce A_2 and B_2 symmetry coordinates, respectively.

In Table 12 the symmetry coordinates of the unit cell are listed in the order in which the symmetry coordinates of a single chain, on which they are based, are illustrated in Figure 9. Each one is described in terms of the displacements which are expected to determine its frequency, and consequently a crude estimate is made of the expected vibrational frequencies. As a guideline for making these estimates, hydrogen-bond stretching modes were assumed to occur near 200 cm^{-1} , mixed hydrogen bond bending and stretching modes were assumed to occur between 100 and 200 cm^{-1} , hydrogen bond bending modes were assumed to occur between 50 and 100 cm^{-1} and interchain vibrations, involving movement of one chain with respect to the other in the unit cell, were assumed to occur between about 30 and 70 cm^{-1} .

One can extend the descriptions and frequency

Table 12. Symmetry coordinates of acetic acid I

Coordinate	Symmetry under C _{2v}	Single chain Coordinate	Description	Estimated Frequency (cm ⁻¹)
1	A ₁	S ₁ (A')	hydrogen bond stretch & bend	150±50
2	B ₁	S ₁ (A')	hydrogen bond stretch & bend	150±50
3	A ₁	S ₂ (A')	hydrogen bond bend & stretch	150±50
4	B ₁	S ₂ (A')	hydrogen bond bend & stretch	150±50
5	A ₁	S ₃ (A')	hydrogen bond bend	75±25
6	B ₁	S ₃ (A')	hydrogen bond bend	75±25
7	A ₁	S ₄ (A')	hydrogen bond bend	75±25
8	B ₁	S ₄ (A')	hydrogen bond bend	75±25
9	A ₁	S ₅ (A')-S ₆ (A')	Translation of unit cell along c	0
10	B ₁	S ₅ (A')	van der Waals' forces	<70
11	A ₁	S ₆ (A')	van der Waals' forces	<70
12	B ₁	S ₆ (A')+S ₅ (A')	Translation of unit cell along	0

(Table continued)

Table 12 continued

Coordinate	Symmetry under C_{2v}	Single chain Coordinate	Description	Estimated Frequency (cm^{-1})
13	A_2	$S_7(A'')$	hydrogen bond stretch & bend	150±50
14	B_2	$S_7(A'')$	hydrogen bond stretch & bend	150±50
15	A_2	$S_8(A'')$	hydrogen bond stretch & bend	150±50
16	B_2	$S_8(A'')$	hydrogen bond stretch & bend	150±50
17	A_2	$S_9(A'')$	hydrogen bond bend	75±25
18	B_2	$S_9(A'')$	hydrogen bond bend	75±25
19	A_2	$S_{10}(A'')$	hydrogen bond bend	75±25
20	B_2	$S_{10}(A'')$	hydrogen bond bend	75±25
21	A_2	$S_{11}(A'')$	hydrogen bond bend	75±25
22	B_2	$S_{11}(A'')$	hydrogen bond bend	75±25
23	A_2	$S_{12}(A'')$	van der Waals' forces	<70
24	B_2	$S_{12}(A'')$	Translation of unit cell along a	0

estimates given in Table 12 somewhat, in the following way. S_1 to S_4 are expected to interact to yield two normal vibrations, of symmetry $A_1 + B_1$, near to 200 cm^{-1} and two, of symmetry $A_1 + B_1$, near to, but probably above, 100 cm^{-1} . S_{14} and S_{16} are expected to interact to yield one vibration near to 200 cm^{-1} and one near to 100 cm^{-1} . Further S_5 , S_6 , S_{18} , and S_{20} are expected to have higher frequencies than S_7 , S_8 and S_{22} . Thus a very approximate prediction is that three vibrations absorb near to 200 cm^{-1} , three absorb near to but above 100 cm^{-1} , four absorb near to but below 100 cm^{-1} , three absorb near to 70 cm^{-1} and two absorb between 30 and 70 cm^{-1} .

5B. Far Infrared Spectra Obtained

Far infrared spectra of acetic acid I, acetic acid II and propionic acid at about -180°C (93°K) were obtained between 360 and about 20 cm^{-1} using the methods described in Section 2E. The spectra are presented in Figures 10 to 12, and the frequencies of the observed features are given in Table 13.

The spectrum of acetic acid I shown in Figure 10 was obtained in two sections. The spectrum from 350 to 70 cm^{-1} was obtained as the average of twelve spectra

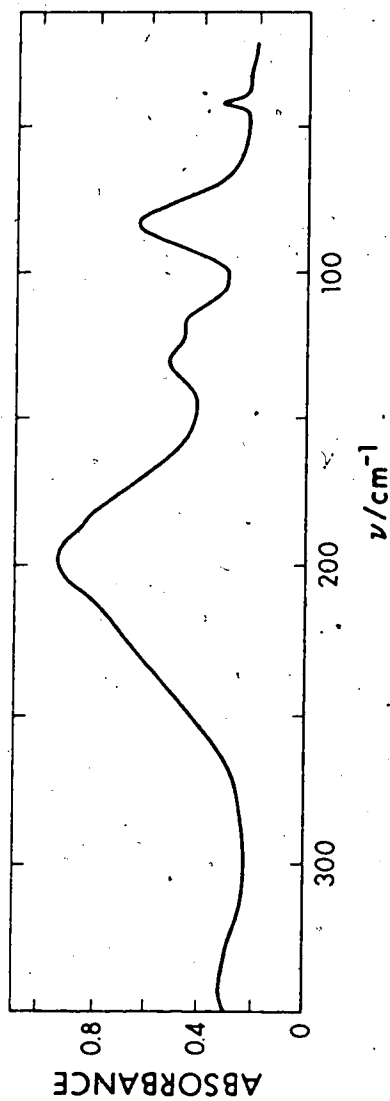


Figure 10. The far infrared spectrum of polycrystalline acetic acid I at approximately -180°C .

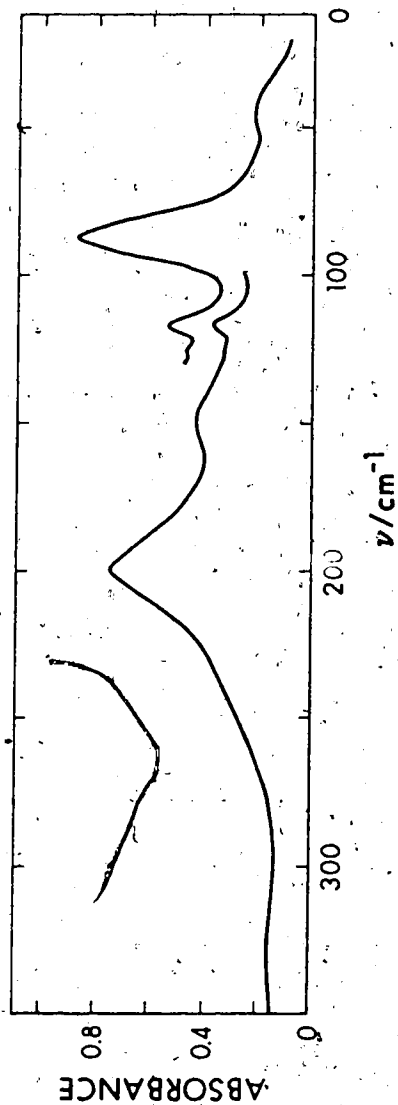


Figure 11. The far infrared spectrum of polycrystalline acetic acid II at approximately -180°C

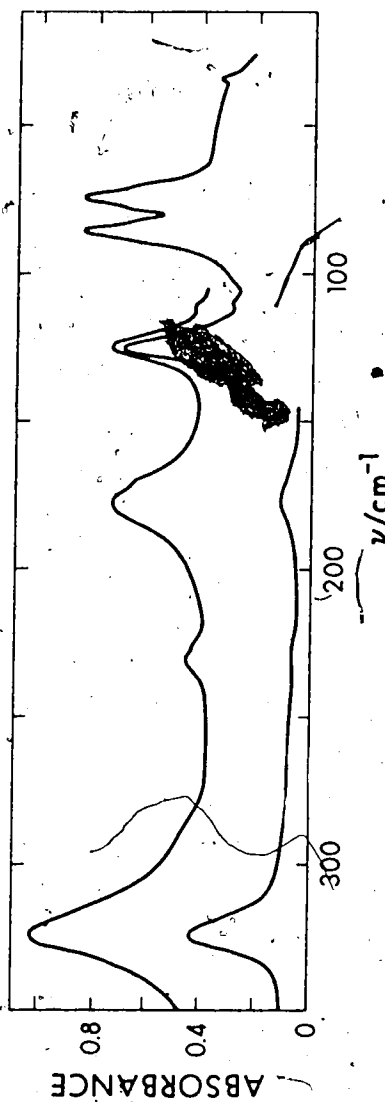


Figure 12. The far infrared spectrum of polycrystalline propionic acid at approximately -180°C . The low-frequency curve has been lowered by 0.05 units for clarity.

Table 13. Observed Vibrational Frequencies of Acetic Acid I, Acetic Acid II and Propionic Acid. vs - very strong, s - strong, m - medium, w - weak and vw - very weak.

Acetic Acid I		Acetic Acid II		Propionic Acid	
Frequency (cm^{-1})	Description	Frequency (cm^{-1})	Description	Frequency (cm^{-1})	Description
341±2	m; broad	333±5	vw; very broad	323±1	vs; sharp
230	w; shoulder	245	w; shoulder	290±3	w; broad
197±2	vs; broad	200±1	vs; broad	230±1	w
183	vw; shoulder	147±1	m; broad	225	vw; shoulder
130±1	m	125.0±0.5	vw	177±1	s
116±1	w	116.0±0.5	w; sharp	170	vw, shoulder
83±1	s; sharp	86.0±0.5	s; sharp	124.5±0.5	s; sharp
43.0±0.5	vw; sharp			111.0±0.5	vw
				85.0±0.5	s; sharp
				73.0±0.5	s; sharp
				34.0±0.5	vw; sharp

of three different samples and the spectrum from 100 to 20 cm^{-1} is the average of 10 spectra of three samples. Both curves have been smoothed to remove non-reproducible features which had an order of magnitude similar to that of the width of the line used to draw the curves. The two sections of the spectrum obtained in this way matched perfectly in the overlap region so they have been drawn as a continuous line in Figure 10.

The main uncertainty in the spectrum is that it is possible that the absorption between 180 and 220 cm^{-1} should be slightly more intense and, therefore, the feature in this region should appear less flat-topped than it does. Further, other features of comparable magnitude to the peak at 43 cm^{-1} appeared near to it in some of the averaged spectra obtained, but the 43 cm^{-1} feature was the only reproducible one and, therefore, is believed to be the only real feature in that region. The spectrum reported is consistent with those reported previously, apart from small frequency and relative intensity differences, but shows significantly more detail, partly because of the greater continuous frequency range. The features at 341, 230 and 183 cm^{-1} have not been reported before, although a suggestion of the latter shoulder is visible in

Stanevich's spectra (51). The doublet feature at $130/116\text{ cm}^{-1}$ was previously reported as a single peak (1) and the previous report of the peak at 43 cm^{-1} indicated that its intensity relative to that of the peak at 83 cm^{-1} was much greater (51) than that found in this work.

The higher-frequency part of the spectrum of acetic acid II shown in Figure 11 is the average of thirteen spectra of three samples while the lower-frequency part is the average of seventeen spectra of five samples which were more strongly absorbing than those used for the higher frequencies. Both parts of the spectrum have been smoothed to remove non-reproducible features whose magnitude was of the order of the width of the line used to draw the curves. The only uncertainty in the spectrum lies in the broad weak feature near 40 cm^{-1} which showed significant variation in its relative intensity and therefore, may not be real.

The spectrum of propionic acid is shown in Figure 12. The upper spectrum between 110 and 350 cm^{-1} is the average of fifteen spectra of four samples while the spectrum between 140 and 20 cm^{-1} is the average of nine spectra of three samples and has been lowered by

0.05 units for clarity. Both curves have been smoothed to eliminate non-reproducible features of the order of magnitude of the width of the line used.

The number of features present below 60 cm^{-1} is somewhat uncertain. The peak shown at 34 cm^{-1} was reproducible in all spectra, while other features which were of comparable size on this average spectrum were not present on other averages and have, therefore, been removed from the spectrum shown. Similarly the shoulders at 225 and 170 cm^{-1} are believed to be real, but, because they are so weak, they could be spurious. There is also some uncertainty in the position of zero absorbance for these two curves because the peak at 124.5 cm^{-1} is stronger relative to the background absorption in the lower-frequency curve than in the higher-frequency curve whereas the background absorption is greater in the higher-frequency curve. Therefore it seems probable that the nearly flat background absorption should be much nearer to zero absorbance than is shown in Figure 12.

The lower curve between 110 and 350 cm^{-1} is the smoothed average of three spectra of a weakly absorbing sample. It is included to show that the peak at 323 cm^{-1} is significantly more intense relative to the one at 177 cm^{-1} than is apparent from the spectrum with higher

absorbance.

The propionic acid spectrum obtained here is similar to those reported previously (51,69,70) apart from small frequency differences, but shows more detail. Thus the doublet absorption at 85 and 73 cm^{-1} has previously been reported as a single peak at 77 - 78 cm^{-1} (51,69,70) and the features at 111, 170 and 225 cm^{-1} have not been reported previously. A peak at 230 cm^{-1} was reported to have varying relative intensity and was thought to be due to ice (69,70). However, spectra of the mulling agent, propane, were obtained using identical techniques to those used for the spectra of the acids mulled in propane, and showed no sign of absorption by ice. Thus, it is believed, that the weak absorption at 230 cm^{-1} and the shoulder at 225 cm^{-1} are due to propionic acid.

5C. Discussion of the spectra

It is clear from a comparison of the spectrum of acetic acid I (Figure 10) with the approximate predictions made in Section 5A that an unambiguous assignment of the spectrum is impossible at the present time, but that vibrations are expected in all regions where significant absorption is observed. It is fairly certain

that the peaks near 200, 125, 83 and 43 cm^{-1} arise from vibrations which involve hydrogen bond stretching, a mixture of hydrogen bond stretching and bending, hydrogen bond bending and interchain displacements, respectively. A more detailed assignment must await the results of infrared or Raman studies on single crystals of acetic acid I which can unambiguously characterize the symmetry of the vibration causing a peak.

A striking feature of the acetic acid I spectrum that has not been reported previously is the breadth of the absorption centered at 197 cm^{-1} . Its width at half the peak intensity is about 70 cm^{-1} , compared to the $\sim 5\text{ cm}^{-1}$ half-width which is expected for peaks due to intermolecular vibrations in ordered crystals and which is found in the spectra of the ordered forms of ice (97). Similar very broad features have been observed in the far infrared spectra of the disordered forms of ice (97-100) and the clathrate hydrates (101,102), and have been interpreted as being due to the disorder which results from the two possible positions which the hydrogen atom may occupy in the hydrogen bond (98,103). The only significant disorder of this type that can be envisaged in the acetic acid I structure is the possibility that there is no correlation between the positions of the hydrogen-bonded hydrogen atoms in different chains. Such

disorder, however, should have been detected in the neutron diffraction study (27), and in the X-ray study (18,19) because it involves the interchange of C=O and C-O bonds. It must be concluded therefore, that acetic acid I is not significantly disordered in this way, although the diffraction studies would probably not have detected disorder in about 5% of the chains (104).

It is probable, therefore, that the extremely broad band in the spectrum of acetic acid I is not due to disorder. A source of breadth of absorption by ordered solids is the overlapping of bands due to several zero-wave-vector vibrations. It was shown, however, in Section 5A that only 4 such vibrations are expected between 150 and 200 cm^{-1} , so the broad band in the spectrum of acetic acid I can not be due to this cause and its origin must remain unknown until further evidence is available.

The assignment of the spectrum of propionic acid (Figure 12) is now considered with the help of Tables 5 and 6 (Section 1D). Again it is not possible to make an unambiguous assignment from the data available. The doublet at 73/85 cm^{-1} may be due to the two active components of ν_4 (Table 5) or may be due to one or both components of ν_4 and ν_5 , because the 40 cm^{-1} frequency assigned by Stanevich (51) to ν_5 seems very low for this vibration. The absorption at 34 cm^{-1} is assigned to one

of the three active translational vibrations of the dimers. The features at 177 and 170 cm^{-1} can be assigned to the two components of ν_3 , and the peaks at 323 and 124.5 cm^{-1} are assigned to intramonomer modes following Jakobsen *et. al.* (69) and Mikawa *et. al.* (70), (Table 6). The assignment of the remaining four weak features at 290, 230, 225 and 111 cm^{-1} is less clear. The only one whose frequency is near to that expected for an unassigned fundamental transition is at 111 cm^{-1} and it is extremely weak. All four features can be assigned to combination transitions, and until more evidence is available further speculation is pointless.

Since the assignments of the spectra of acetic acid I and propionic acid, whose crystal structures are known, are limited; it seems clear that a detailed assignment of the spectrum of acetic acid II is impossible. However, it can definitely be concluded that acetic acid II consists of hydrogen bonded monomers because of the high frequencies at which the inter-monomer vibrations occur. One can also attempt to deduce whether acetic acid II consists of polymeric chains or dimers from a comparison of its spectrum with those of acetic acid I and propionic acid. The peaks at 124.5 and 323 cm^{-1} in the spectrum of propionic acid must be excluded from the comparison because they are due to the ethyl group.

It can be observed that the long-chain structure of acetic acid I yields an extremely broad absorption near 200 cm^{-1} which is continuous with weak absorptions near 125 cm^{-1} , while the dimeric structure of propionic acid yields much sharper absorption lines which are distinct from each other. A further observation is that the hydrogen bond stretching vibrations absorb near 180 cm^{-1} in the dimeric structure while the absorption maximum due to hydrogen bond stretching modes in the long-chain structure is near 200 cm^{-1} . The reasons for these differences are unknown and hence one can not be sure that they are a reliable way of distinguishing between the two structures. Nevertheless, the spectrum of acetic acid II is very similar to that of acetic acid I and, from the evidence available at present, it can be concluded that acetic acid II probably consists of hydrogen-bonded chains of acetic acid molecules. The molecular volume of acetic acid II is smaller than that of acetic acid I and it is probable that the main difference between the two structures is a closer packing of the chains in acetic acid II than in acetic acid I.


5D. Summary and Conclusions

(1) the pressure-temperature phase diagram of acetic acid has been measured volumetrically between 0

and -40°C to 3 Kbar. The acetic acid I \rightarrow II phase transition involves a $0.014\text{ cm}^3/\text{g}$ decrease in volume. Acetic acid II cannot be formed from acetic acid I below about 800 bar, even though it appears to be the stable phase at one atmosphere below about -60°C . Once formed, though, acetic acid II is metastable at one atmosphere below about -35°C .

(2) The X-ray diffraction pattern of powdered acetic acid II has been obtained and indexed on a monoclinic cell with the dimensions: $a = 13.30 \pm 0.02\text{ \AA}$, $b = 10.39 \pm 0.01\text{ \AA}$, $c = 8.59 \pm 0.01\text{ \AA}$, and $\beta = 86.1 \pm 0.3^{\circ}$ at 100°K and atmospheric pressure. If the unit cell contains 16 molecules, the molar volume is $44.6\text{ cm}^3/\text{mole}$, 1.5% smaller than that of acetic acid I, which is in agreement with the results from the phase diagram work.

(3) The far infrared spectrum of acetic acid II has been obtained and compared with those of acetic acid I and propionic acid. It has been argued that acetic acid II probably consists of hydrogen-bonded chains of monomers which are packed in a more efficient way than in acetic acid I.



References

1. R. J. Jakobsen, Y. Mikawa, and J. W. Brasch, *Spectrochimica Acta*, 23A, 2199 (1967)
2. G. Tammann, *Kristallisieren und Schmelzen*, page 275 (1903)
3. P. W. Bridgman, *Proc. Amer. Acad. Sci.*, 52, 91 (1916)
4. L. Deffet, *Bull. Soc. Chim. Belg.*, 44, 41 (1935)
5. *Handbook of Physics and Chemistry*, 50th edition, The Chemical Rubber Company, Cleveland (1970)
6. Willy Tan, K. A. Krieger, and John G. Miller, *J. Am. Chem. Soc.*, 74, 6181 (1952)
7. R. Philippe and A. M. Piette, *Bull. Soc. Chim. Belg.*, 64, 600 (1955)
8. L. Raczy, E. Constant, and R. Gabillard, *Compt. Rend.*, 252, 2523 (1961)
9. J. Timmermans, and M. Kasanin, *Bull. Soc. Chim. Belg.*, 68, 527 (1959)
10. R. J. Jakobsen and J. E. Katon, *Developments in Applied Spectroscopy*, Vol. 10, page 107, Plenum Publishing Corporation, New York, 1972
11. *Beilsteins Handbuch*, published by Julius Springer, Berlin (1920), reproduced by Edwards Brothers, Inc., Ann Arbor, Michigan (1943), Volume 2, page 99

Beilsteins Handbuch, published by Julius Springer, Berlin (1929), reproduced by Edwards Brother, Inc., Ann Arbor, Michigan (1942), Volume 2, Supplement 1, page 41

Beilsteins Handbuch, Springer-Publishing House, Berlin (1942), reproduced by Edwards Brothers Inc., Ann Arbor, Michigan (1943), Volume 2, Supplement 2, page 97

Beilsteins Handbuch, Springer-Publishing House, Berlin (1960) Volume 2, Supplement 3, page 143.
12. J. Timmermans, *Physico-Chemical Constants of Pure Organic Compounds*, Elsevier Publishing Company, Inc., New York, Volume 1, page 380-383 (1950)
 Volume 2, page 277-279 (1965)

13. W. R. Bousfield and T. M. Lowry, J. Chem. Soc. (London), 99, 1432 (1911)
14. W. C. Eichelberger and V. K. La Mer, J. Am. Chem. Soc., 55, 3633 (1933)
15. C. Schall and C. Thieme-Wiedtmarckter, Zeitschrift fur Electrochemie und Angewandte Physikalische Chemie, 35, 337 note 3 (1929).
16. S. Young, Sci. Proc. Soc. Dublin, N. S. XII, 374 (1909-10)
17. J. M. Costello and S. T. Bowden, Rec. Trav. Chim., 77, 803 (1958)
18. I. Nahringsbauer, Acta Chem. Scand., 24, 453 (1970)
19. R. E. Jones and D. H. Templeton, Acta Cryst., 11, 484 (1958).
20. D.A. MacInnes and T. Shedlovsky, J. Am. Chem. Soc., 54, 1429 (1932).
21. H. F. Hall and H. H. Voge, J. Am. Chem. Soc., 55, 239 (1933)
22. J. Kendall and P.M. Gross, J. Am. Chem. Soc., 43, 1426 (1921).
23. R. J. W. Le Fevre, Trans. Faraday Soc., 34, 1127 (1938)
24. E. Constant and A. Lebrun, J. Chim. Phys., 61 (1-2), 163 (1964)
25. N. A. Puschin and P. G. Matavulj, Z. Physik. Chem., A161, 341 (1932)
26. R. R. Driesbach and R. A. Martin, Ind. Eng. Chem., 41, 2875 (1949)
27. P-G. Jonsson, Acta Cryst., B27, 893 (1971)
28. T. E. Thorpe and J. W. Rodger, Phil. Trans., 185A, 397 (1894)
29. M. Hennaut-Roland and L. Lek, Bull. Soc. Chim. Belg., 40, 177 (1931)
30. F. Schwerts, Bull. Cl. Sci. Acad. Roy. Belg., 731 (1912)

31. F. Von Rautenfeld and E. Steurer, Z. Physik. Chem., 51B, 39 (1942)
32. M. L. E. O. De Visser, Thesis, Utrecht (1891) and Rec. Trav. Chim., 12, 101 (1893)
33. G. S. Parks and K. K. Kelly, J. Am. Chem. Soc., 47, 2089 (1925)
34. Dow Chemical Company, unpublished (1956)
35. J. Meyer, Z. Physik. Chem., 72, 225 (1910)
36. O. Pettersson, Jour. Prak. Chem. (2), 24, 296
37. G. Massol and M. Guillot, Compt. Rend., 121, 208 (1895).
38. M. Haurie and A. Novak, J. Chim. Phys., 62, 137 (1965)
39. W. Weltner, J. Am. Chem. Soc., 77, 3911 (1955)
40. J. R. Wilmshurst, J. Chem. Phys., 6, 1171 (1956)
41. P. Waldstein and L. A. Blatz, J. Phys. Chem., 71, 2271 (1967)
42. J. L. Derissen, J. Mol. Struct., 7, 67 (1971)
43. J. Donohue, Acta Cryst., B24, 1558 (1968) and references therein
44. M. Haurie and A. Novak, J. Chim. Phys., 62, 146 (1965)
45. M. Haurie and A. Novak, J. Chim. Phys., 63, 1584 (1967)
46. E. B. Wilson, Jr., J. C. Decius and P. C. Cross, Molecular Vibrations, McGraw-Hill Book Company, 1955 (New York), page 117
47. T. Miyazawa and K. S. Pitzer, J. Am. Chem. Soc., 81, 74 (1959)
48. R. C. Millikan and K. S. Pitzer, J. Am. Chem. Soc., 80, 3515 (1958)
49. L. Bonner and J. S. Kirby-Smith, Phys. Rev., 57, 1078 (1940)
50. Y. Nakai and K. Hirota, J. Chem. Soc. Japan, 81, 881 (1960)

51. A. E. Stanevich, Optics and Spectroscopy, Supplement 2, 104 (1963)
52. A. E. Stanevich, Optics and Spectroscopy, 16, 243 (1964)
53. U. A. Zirnit and M. M. Sushchinskii, Optics and Spectroscopy, 16, 490 (1964)
54. S. Kishida and K. Nakamoto, J. Chem. Phys., 41, 1558 (1964)
55. G. L. Carlson, R. E. Witkowski and W. G. Fateley, Spectrochimica Acta, 22, 1117 (1966)
56. S. G. W. Ginn and J. L. Wood, J. Chem. Phys., 46, 2735 (1967)
57. R. Fauquembergue, E. Constant and L. Racz, Compt. Rend., Series C, 264, 1325 (1967)
58. J. E. Saunders, F. F. Bentley and J. E. Katon, Applied Spectroscopy, 22, 286 (1968)
59. K. Fukishima and B. J. Zwolinski, J. Chem. Phys., 50, 737 (1969)
60. A. Witkowski, J. Chem. Phys., 52, 4403 (1970)
61. Y. Marechal and A. Witkowski, J. Chem. Phys., 48, 3697 (1968)
62. R. L. Redington and R. C. Lin, J. Chem. Phys., 54, 4111 (1971)
63. Y. Grenie, J-C. Cornut and J-C. Lassegues, J. Chem. Phys., 55, 5844 (1971)
64. J. E. Bertie and J. W. Bell, J. Chem. Phys., 54, 160 (1971)
65. T. Shimanouchi, M. Tsuboi and T. Miyazawa, J. Chem. Phys., 35, 1597 (1961)
66. E. B. Wilson, J. C. Decius and P. C. Cross, Molecular Vibrations, McGraw Hill Book Company, 1955 (New York), page 113
67. M. Haurie and A. Novak, Spectrochimica Acta, 21, 1217 (1965)
68. F. J. Stieter, D. H. Templeton, R. F. Scheuerman and R. L. Sass, Acta Cryst., 15, 1233 (1962)

69. R. J. Jakobsen, Y. Mikawa and J. W. Brasch, *Spectrochimica Acta*, 25A, 839 (1969)
70. Y. Mikawa, J. W. Brasch and R. J. Jakobsen, *J. Mol. Structure*, 3, 103 (1969)
71. R. J. Jakobsen, Y. Mikawa, J. R. Allkins and G. L. Carlson, *J. Mol. Structure*, 10, 300 (1971)
72. K. Fischer, *Angew. Chem.*, 48, 394 (1935)
73. E. D. Peters and J. L. Jungnickel, *Anal. Chem.*, 37, 450 (1950)
74. J. Timmermans, "The Physico-chemical Constants of Binary Systems in Concentrated Solutions", Vol. 4, Interscience Publishers, Inc., New York, (1960), pages 355-376
75. P. W. Bridgman, *Proc. Am. Acad. Sci.*, 51, 59 (1915)
76. H. Schildknecht, *Z. Anal. Chem.*, 181, 254 (1961)
77. S. R. Gough and D. W. Davidson, *J. Chem. Phys.*, 52, 5442 (1970)
78. J. E. Bertie and P. Tremaine, *J. Chem. Phys.*, 58, 854 (1973)
79. G. S. Kell and E. Whalley, *J. Chem. Phys.*, 48, 2359 (1968)
80. E. W. Nuffield, "X-Ray Diffraction Methods", John Wiley and Sons, Inc., New York (1966), page 34
81. R. W. M. D'Eye and E. Wait, "X-Ray Powder Photography in Inorganic Chemistry", Butterworths Scientific Publications, London (1960), page 24
82. I. Waller and R. W. James, *Proc. Roy. Soc. (London)*, 117A, 214 (1927)
83. R. Brill and A. Tippe, *Acta Cryst.*, 23, 343 (1967)
84. J. E. Bertie and E. Whalley, *Spectrochim. Acta*, 20, 1349 (1964)
85. A. E. Marfin, "Infrared Instrumentation and Techniques", Elsevier Publishing Company, Amsterdam (1966), page 118 and RIIC Instruction Manual for the Fourier Spectrophotometer FS-720 (1967), page 8, Research and Industrial Instruments Company, London

86. A. E. Martin, "Infrared Instrumentation and Techniques", Elsevier publishing Company, Amsterdam (1966)
87. S. Sunder, Ph.D. Thesis, University of Alberta (1972)
88. G. Horlick, Analytical Chemistry, 43, 61A, (1971)
89. M. Solinas, Ph.D. Thesis, University of Alberta (1973)
90. J.E. Bertie and P. Tremaine, J. Chem. Phys., 58, 854 (1973)
91. S.E. Babb, High Pressure Measurement, edited by A.A. Gardini and E.C. Lloyd, Butterworths, Washington, D.C., 1962, page 115
92. R.S. Dadson and R.G.P. Greig, Br. J. Appl. Phys., 16, 1711 (1965).
93. R. Hesse, Acta Cryst., 1, 200 (1948).
94. H. Lipson, Acta Cryst., 2, 43 (1949)
95. K. Simpson, Ph.D. Thesis, The University of Alberta (1973).
96. P. Tremaine, Ph.D. Thesis, The University of Alberta (1974).
97. J.E. Bertie and E. Whalley, J. Chem. Phys., 41, 775 (1968).
98. J.E. Bertie, Applied Spectroscopy, 22, 634 (1968).
99. J.E. Bertie and E. Whalley, J. Chem. Phys., 46, 1271 (1967).
100. J.E. Bertie, H.J. Labbé and E. Whalley, J. Chem. Phys., 49, 2141 (1968).
101. J.E. Bertie and D.A. Othen, Can. J. Chem., 50, 3443 (1972).
102. J.E. Bertie and D.K. Hendricksen, unpublished.
103. E. Whalley and J.E. Bertie, J. Chem. Phys., 46, 1264 (1967).
104. M.J. Bennett, private communication.